JOURNAL OF OPTIMIZATION THEORY AND APPLICATIONS: Vol. 49, No. 1, APRIL 1986

Optimal Take-Off Trajectories in the Presence of Windshear[1,2,3]

A. MIELE,[4] T. WANG,[5] AND W. W. MELVIN[6]

Abstract. This paper is concerned with optimal flight trajectories in the presence of windshear. With particular reference to take-off, eight fundamental optimization problems [Problems (P1)-(P8)] are formulated under the assumptions that the power setting is held at the maximum value and that the airplane is controlled through the angle of attack.

Problems (P1)-(P3) are least-square problems of the Bolza type. Problems (P4)-(P8) are minimax problems of the Chebyshev type, which can be converted into Bolza problems through suitable transformations. These problems are solved employing the dual sequential gradient-restoration algorithm (DSGRA) for optimal control problems.

Numerical results are obtained for a large number of combinations of performance indexes, boundary conditions, windshear models, and windshear intensities. However, for the sake of brevity, the presentation of this paper is restricted to Problem (P6), minimax $|\Delta h|$, and Problem (P7), minimax $|\Delta\gamma|$. Inequality constraints are imposed on the angle of attack and the time derivative of the angle of attack.

The following conclusions are reached: (i) optimal trajectories are considerably superior to constant-angle-of-attack trajectories; (ii) optimal trajectories achieve minimum velocity at about the time when the windshear ends; (iii) optimal trajectories can be found which transfer an aircraft from a quasi-steady condition to a quasi-steady condition through a windshear; (iv) as the boundary conditions are relaxed, a

[1] Portions of this paper were presented at the AIAA Atmospheric Flight Mechanics Conference, Snowmass, Colorado, August 19-21, 1985. The authors are indebted to Boeing Commercial Aircraft Company, Seattle, Washington and to Pratt and Whitney Aircraft, East Hartford, Connecticut for supplying some of the technical data pertaining to this study.

[2] This research was supported by NASA-Langley Research Center, Grant No. NAG-1-516. The authors are indebted to Dr. R. L. Bowles, NASA-Langley Research Center, Hampton, Virginia, for helpful discussions.

[3] This paper is based in part on Refs. 1-5.

[4] Professor of Astronautics and Mathematical Sciences, Aero-Astronautics Group, Rice University, Houston, Texas.

[5] Senior Research Associate, Aero-Astronautics Group, Rice University, Houston, Texas.

[6] Captain, Delta Airlines, Atlanta, Georgia; and Chairman, Airworthiness and Performance Committee, Air Line Pilots Association (ALPA), Washington, DC.

0022-3239/86/0400-0001$05.00/0

higher final altitude can be achieved, albeit at the expense of a considerable velocity loss; (v) among the optimal trajectories investigated, those solving Problem (P7) are to be preferred, because the altitude distribution exhibits a monotonic behavior; in addition, for boundary conditions BC2 and BC3, the peak angle of attack is below the maximum permissible value; (vi) moderate windshears and relatively severe windshears are survivable employing an optimized flight strategy; however, extremely severe windshears are not survivable, even employing an optimized flight strategy; and (vii) the sequential gradient-restoration algorithm (SGRA), employed in its dual form (DSGRA), has proven to be a powerful algorithm for solving the problem of the optimal flight trajectories in a windshear.

Key Words. Piloting strategies, flight mechanics, take-off, optimal trajectories, optimal control, windshear problems, sequential gradient-restoration algorithm, dual sequential gradient-restoration algorithm.

1. Introduction

Low-altitude windshear constitutes a considerable hazard in the take-off and landing of both civilian airplanes and military airplanes. For this reason, considerable research has been done on this problem over the past 15 years. Most of the research has been concerned with meteorological studies, instrumentation studies, aerodynamic studies, and stability studies. It appears that the study of the optimal flight trajectories in the presence of a windshear has been overlooked so far. Because flight in a windshear depends critically on the action of the pilot on the controls of the aircraft, the determination of the optimal flight trajectories is of considerable importance.

Previous Research. Previous research on the topics covered in this paper can be found in Refs. 6–37. For a general review of windshear studies, see Ref. 6. For the equations of motion without windshear, see Ref. 7; for the equations of motion with windshear, see Refs. 8–11. For windshear models, see Refs. 12–16.

Concerning trajectory optimization, for a recent overview of theoretical calculus of variations and optimal control, see Ref. 17. For algorithmic optimal control by means of gradient methods, see Refs. 18–22 (primal formulation) and Refs. 23–24 (dual formulation). For minimax optimal control, see Refs. 25–37; in particular, for aerospace applications of minimax optimal control, see Refs. 26 and 33–37.

Present Research. This paper deals with optimal flight trajectories in the presence of windshear. The take-off problem is analyzed. In take-off, once an aircraft becomes airborne, the pilot has no choice but to fly through

a windshear. His only control is the angle of attack. Indeed, it is logical to assume that, if a plane takes off under less-than-ideal weather conditions, the power setting is being held at that value which yields the maximum thrust.

Eight fundamental optimization problems [Problems (P1)-(P8)] are formulated. Among these, Problems (P1)-(P3) are least-square problems of the Bolza type and Problems (P4)-(P8) are minimax problems of the Chebyshev type. These problems are solved numerically employing the dual sequential gradient-restoration algorithm (DSGRA) for optimal control problems. Inequality constraints are imposed on the angle of attack and the time derivative of the angle of attack.

The optimal transfer of an aircraft from a quasi-steady condition to a quasi-steady condition through a windshear is investigated. The effect of the number of final conditions is also investigated. Finally, the effect of the intensity of the windshear is studied in order to assess survivability.

Outline. Section 2 contains the notations, and Section 3 presents the coordinate systems and the equations of motion. The approximations employed for the force terms and the windshear terms are discussed in Sections 4–5. The inequality constraints on α and $\dot{\alpha}$ are presented in Section 6, and the boundary conditions are given in Section 7. The optimal control problems are formulated in Section 8, and the sequential gradient-restoration algorithm is briefly mentioned in Section 9. The data for the examples are presented in Section 10. Finally, the numerical results are discussed in Section 11, and the conclusions are given in Section 12.

2. Notations

Throughout the paper, the following notations are employed:

ARL = aircraft reference line;
D = drag force, lb;
g = acceleration of gravity, ft sec^{-2};
h = altitude, ft;
L = lift force, lb;
m = mass, lb ft^{-1} sec^2;
T = thrust force, lb;
u = auxiliary control variable, (rad)$^{1/2}$;
V = relative velocity, ft sec^{-1};
V_e = absolute velocity, ft sec^{-1};
$W = mg$ = weight, lb;
W = wind velocity, ft sec^{-1};
W_h = h-component of wind velocity, ft sec^{-1};
W_x = x-component of wind velocity, ft sec^{-1};
x = horizontal distance, ft.

Greek Symbols

α = relative angle of attack, rad;
α_e = absolute angle of attack, rad;
β = engine power setting;
γ = relative path inclination, rad;
γ_e = absolute path inclination, rad;
δ = thrust inclination, rad;
θ = pitch attitude angle, rad.

Subscripts

e = denotes Earth-fixed system;
l = denotes direction orthogonal to relative velocity;
le = denotes direction orthogonal to absolute velocity;
h = denotes h-direction;
x = denotes x-direction;
v = denotes direction of relative velocity;
ve = denotes direction of absolute velocity.

Superscripts

$\cdot$ = denotes derivative with respect to time;
$\rightarrow$ = denotes vector quantity.

3. Coordinate Systems and Equations of Motion

In Ref. 1, three coordinate systems were defined: (i) the Earth-fixed system, (ii) the relative wind-axes system, and (iii) the absolute wind-axes system. It was assumed that flight takes place in a vertical plane.

Let $\vec{V}$ denote the velocity of the aircraft with respect to the airstream; let $\vec{W}$ denote the velocity of the airstream with respect to the Earth; and let $\vec{V}_e$ denote the velocity of the aircraft with respect to the Earth. With this understanding, the coordinate systems (i), (ii), (iii) are defined below (see Fig. 1).

In the Earth-fixed system Oxh, the point O is fixed with respect to the Earth; the x-axis is horizontal, positive in the sense of the motion; and the h-axis is orthogonal to the x-axis, hence vertical, positive upward.

In the relative wind-axes system $Px_v y_l$, the point P moves together with the aircraft; the x_v-axis has the direction of the relative velocity vector $\vec{V}$; and the y_l-axis has the direction of the lift vector $\vec{L}$.

In the absolute wind-axes system $Px_{ve}y_{le}$, the point P moves together with the aircraft; the x_{ve}-axis has the direction of the absolute velocity vector

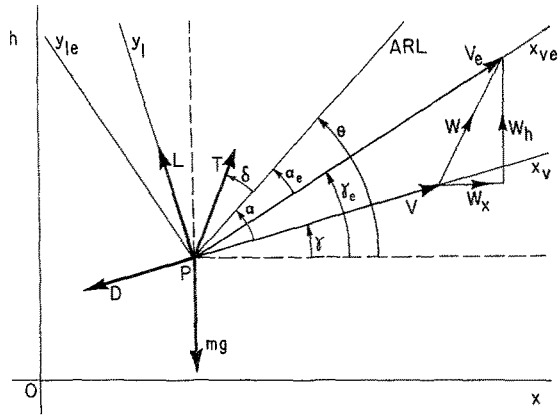

Fig. 1. Coordinate systems and force diagram.

$\vec{V}_e$; and the y_{le}-axis has the direction of the projected lift vector $\vec{L}_e$; the latter vector is obtained by projecting $\vec{L}$ in the direction orthogonal to x_{ve}.

In Ref. 1, the equations of motion under windshear conditions were derived for the above coordinate systems under the following assumptions: (a) the aircraft is a particle of constant mass; (b) flight takes place in a vertical plane; (c) Newton's law is valid in an Earth-fixed system; and (d) the wind flow field is steady.

In this paper, we employ hypotheses (a) through (d) in connection with the equations of motion written for the relative wind-axes system. The reason for preferring (ii) to (i), (iii) is that the windshear terms appear explicitly in (ii) and implicitly in (i), (iii). Hence, if system (ii) is employed, it is easier to understand the dynamical effects associated with the windshear terms.

With the above premises, the equations of motion are written as follows:

$$\dot{x} = V\cos\gamma + W_x, \tag{1a}$$

$$\dot{h} = V\sin\gamma + W_h, \tag{1b}$$

$$\begin{aligned}\dot{V} = {} & (T/m)\cos(\alpha+\delta) - D/m - g\sin\gamma \\ & -[(\partial W_x/\partial x)(V\cos\gamma + W_x) + (\partial W_x/\partial h)(V\sin\gamma + W_h)]\cos\gamma \\ & -[(\partial W_h/\partial x)(V\cos\gamma + W_x) + (\partial W_h/\partial h)(V\sin\gamma + W_h)]\sin\gamma,\end{aligned} \tag{1c}$$

$$\begin{aligned}\dot{\gamma} = {} & (T/mV)\sin(\alpha+\delta) + L/mV - (g/V)\cos\gamma \\ & +[(\partial W_x/\partial x)(V\cos\gamma + W_x) + (\partial W_x/\partial h)(V\sin\gamma + W_h)](1/V)\sin\gamma \\ & -[(\partial W_h/\partial x)(V\cos\gamma + W_x) + (\partial W_h/\partial h)(V\sin\gamma + W_h)](1/V)\cos\gamma.\end{aligned} \tag{1d}$$

These equations must be supplemented by the functional relations

$$D = D(h, V, \alpha), \tag{2a}$$

$$L = L(h, V, \alpha), \tag{2b}$$

$$T = T(h, V, \beta), \tag{2c}$$

$$W_x = W_x(x, h), \tag{2d}$$

$$W_h = W_h(x, h), \tag{2e}$$

and by the analytical relations

$$V_{ex} = V \cos \gamma + W_x, \tag{3a}$$

$$V_{eh} = V \sin \gamma + W_h, \tag{3b}$$

$$V_e = \sqrt{(V_{ex}^2 + V_{eh}^2)}, \tag{3c}$$

$$\gamma_e = \arctan(V_{eh}/V_{ex}), \tag{3d}$$

$$\theta = \alpha + \gamma, \tag{3e}$$

$$\alpha_e = \alpha + \gamma - \gamma_e. \tag{3f}$$

For a given value of the thrust inclination δ, the differential system (1)–(2) involves four state variables (the horizontal distance x, the altitude h, the velocity V, and the relative path inclination γ) and two control variables (the angle of attack α and the power setting β). However, the number of control variables reduces to one (the angle of attack α), if the power setting β is specified in advance.

The quantities defined by the analytical relations (3) can be computed *a posteriori*, once the values of x, h, V, γ, α, β are known. Indeed, V_{ex}, V_{eh}, V_e, γ_e are known functions of the state variables defined by Eqs. (3a)–(3d). Analogously, θ, α_e are known functions of the state variables and the control variables defined by Eqs. (3e)–(3f).

4. Approximations for the Force Terms

In this section, we discuss the approximations employed in the description of the forces acting on the aircraft, namely, the thrust, the drag, the lift, and the weight. Because the trajectories under investigation involve relatively minor variations of the altitude, the air density is assumed to be constant.

Thrust. The thrust T is approximated with the quadratic function

$$T = A_0 + A_1 V + A_2 V^2, \tag{4}$$

where V is the relative velocity and where the coefficients A_0, A_1, A_2 depend on the altitude of the runway, the ambient temperature, and the engine power setting. For given runway altitude, ambient temperature, and engine power setting, the coefficients A_0, A_1, A_2 can be determined with a least-square fit of manufacturer-supplied data over a given interval of velocities.

Drag. The drag D is written in the form

$$D = (1/2) C_D \rho S V^2, \tag{5}$$

where ρ is the air density, S is a reference surface, V is the relative velocity, and C_D is the drag coefficient. In turn, the drag coefficient is approximated with the quadratic function

$$C_D = B_0 + B_1 \alpha + B_2 \alpha^2, \qquad \alpha \leq \alpha_*, \tag{6}$$

where α is the relative angle of attack and where the coefficients B_0, B_1, B_2 depend on the flap setting and the undercarriage position (gear up or gear down). For given flap setting and given undercarriage position, the coefficients B_0, B_1, B_2 can be determined with a least-square fit of manufacturer-supplied data over the interval $0 \leq \alpha \leq \alpha_*$.

Lift. The lift L is written in the form

$$L = (1/2) C_L \rho S V^2, \tag{7}$$

where ρ is the air density, S is a reference surface, V is the relative velocity, and C_L is the lift coefficient. In turn, the lift coefficient is approximated as follows:

$$C_L = C_0 + C_1 \alpha, \qquad \alpha \leq \alpha_{**}, \tag{8a}$$

$$C_L = C_0 + C_1 \alpha + C_2 (\alpha - \alpha_{**})^2, \qquad \alpha_{**} \leq \alpha \leq \alpha_*, \tag{8b}$$

where α is the relative angle of attack and where the coefficients C_0, C_1, C_2 depend on the flap setting and the undercarriage position (gear up or gear down). For given flap setting and given undercarriage position, the coefficients C_0, C_1 can be determined with a least-square fit of manufacturer-supplied data over the interval $0 \leq \alpha \leq \alpha_{**}$. With C_0, C_1 known, the coefficient C_2 is determined with a least-square fit of manufacturer-supplied data over the interval $\alpha_{**} \leq \alpha \leq \alpha_*$.

Weight. The mass m is regarded to be constant. Hence, the weight $W = mg$ is regarded to be constant.

5. Approximations for the Windshear

In this section, we discuss some of the approximations employed in the description of the windshear. We observe that, under the assumption that the wind flow field is steady, the wind components W_x, W_h have the form

$$W_x = W_x(x, h), \qquad W_h = W_h(x, h). \tag{9}$$

Windshear Models. Over the past several years, considerable attention has been given to the study of a severe meteorological condition known as a microburst (Refs. 6 and 8–16). This condition involves a descending column of air, which then spreads horizontally in the neighborhood of the ground. This condition is hazardous, because an aircraft in take-off or landing might encounter a headwind coupled with a downdraft, followed by a tailwind coupled with a downdraft. A qualitative example of the vertical cross section of a microburst is shown in Fig. 2.

It is clear that, in order to perform realistic analyses of take-off and landing under severe meteorological conditions, one must represent wind flow fields of the type shown in Fig. 2. The representation of the wind flow field can be obtained from the combination of theory and experimental measurements.

From an engineering point of view, a simplifying observation can be made. In the neighborhood of the ground, the vertical component of the wind velocity is small by comparison with the horizontal component (Ref. 16). Therefore, the idea arises of studying take-off and landing in the presence of windshear by considering only the horizontal component of the wind velocity. This simplified wind model is represented by

$$W_x = W_x(x), \qquad W_h = 0 \tag{10}$$

and is shown in Figs. 3–4. Figure 3 is an idealization of the near-the-ground behavior of the microburst model shown in Fig. 2. In turn, Fig. 4 is a particular case of Fig. 3.

Smoothing Technique. Inspection of Eqs. (1) shows that the first derivatives of the wind components are present in the dynamical equations. Therefore, if gradient-type algorithms are used to optimize flight trajectories in the presence of windshear (Refs. 18–24), one needs the second derivatives of the wind components. For the idealized wind models considered in Figs. 3–4, the first derivatives are discontinuous at the corner points; therefore, the second derivatives do not exist at these points. In the real world, this situation is not acceptable. This being the case, we introduce a smoothing technique designed to ensure the continuity of both the first derivatives and the second derivatives of the wind components.

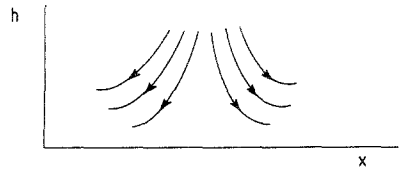

Fig. 2. Typical cross section of the wind flow field (microburst).

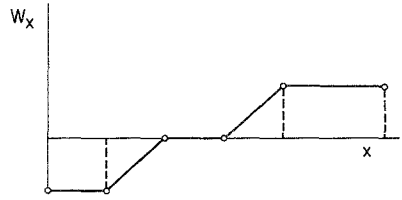

Fig. 3. Idealized distribution of the horizontal component of the wind velocity (W_x positive for tailwind, negative for headwind).

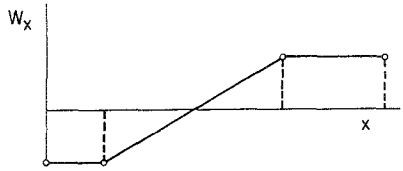

Fig. 4. Idealized distribution of the horizontal component of the wind velocity (W_x positive for tailwind, negative for headwind).

Let the first of Eqs. (10) be written in the general form

$$f = f(x), \tag{11}$$

and assume that a corner point exists at $x = x_0$. Let x_1, x_4 denote two abscissas bracketing the corner point x_0, and let x_2, x_3 denote two intermediate abscissas such that

$$x_4 - x_3 = x_3 - x_2 = x_2 - x_1 = H, \tag{12a}$$

$$x_3 - x_0 = x_0 - x_2 = H/2. \tag{12b}$$

In the interval $x_1 \leq x \leq x_4$, we wish to replace the function (11) with the following triplet of cubic functions:

$$f_1 = f_1(x), \qquad x_1 \leq x \leq x_2, \tag{13a}$$

$$f_2 = f_2(x), \qquad x_2 \leq x \leq x_3, \tag{13b}$$

$$f_3 = f_3(x), \qquad x_3 \leq x \leq x_4. \tag{13c}$$

Each cubic function involves 4 undetermined coefficients, so that the total number of undetermined coefficients is 12. Then, these 12 coefficients are determined in such a way that the continuity of the functions, the first derivatives, and the second derivatives is ensured at x_1, x_2, x_3, x_4. The details of this analysis can be found in Ref. 2. They are omitted here, for the sake of brevity.

If the wind model involves several corner points, the above smoothing technique must be employed at each corner point.

6. Inequality Constraints

The angle of attack α appearing in Eqs. (1), (2), (3), (6), (8) is subject to the inequality

$$\alpha \leq \alpha_*, \tag{14}$$

where α_* is a prescribed upper bound. This inequality constraint can be converted into an equality constraint by means of the Valentine transformation

$$\alpha = \alpha_* - u^2. \tag{15}$$

Here, u denotes an auxiliary control variable.

In addition, the time derivative of the angle of attack is subject to the inequality

$$-C \leq \dot{\alpha} \leq +C, \tag{16}$$

where C is a prescribed, positive constant. To account for Ineq. (16), both α and u must be transformed into state variables. This is done through the introduction of the auxiliary differential equations

$$\dot{\alpha} = C \sin w, \qquad |u| \geq \varepsilon, \tag{17a}$$

$$\dot{\alpha} = C \sin^2(\pi u/2\varepsilon) \sin w, \qquad |u| \leq \varepsilon, \tag{17b}$$

and

$$\dot{u} = -(C/2u) \sin w, \qquad |u| \geq \varepsilon, \tag{18a}$$

$$\dot{u} = -(C/2u) \sin^2(\pi u/2\varepsilon) \sin w, \qquad |u| \leq \varepsilon. \tag{18b}$$

Here, w is an auxiliary control variable and ε is a small, positive constant, which is introduced to prevent the occurrence of singularities.

It must be noted that the right-hand sides of Eqs. (17)–(18) are continuous and have continuous first derivatives at $|u| = \varepsilon$. It must also be noted that Eqs. (17)–(18) imply that

$$\dot{\alpha} = -2u\dot{u}. \tag{19}$$

Hence, (15) is a first integral of (19). This being the case, one has two options: (i) one can supplement the system (1) with both Eqs. (17) and (18); in this case, Eq. (15) must be accounted for only at the initial point; or (ii) one can supplement the system (1) with only Eqs. (18); in this case, Eq. (15) must be accounted for everywhere along the interval of integration; this is easily done through a substitution technique. The second option is simpler than the first and is employed in the subsequent portions of this paper.

7. Boundary Conditions

Concerning the initial conditions, it is assumed that the values of x, h, V, γ, α are specified at $t=0$, that is,

$$x(0)=x_0, \qquad h(0)=h_0, \qquad V(0)=V_0, \qquad \gamma(0)=\gamma_0, \tag{20a}$$

$$\alpha(0)=\alpha_0. \tag{20b}$$

Upon combining (15) and (20b), we see that the specification of the initial value of α implies the specification of the initial value of u, that is,

$$u(0)=u_0=\sqrt{(\alpha_*-\alpha_0)}. \tag{20c}$$

Concerning the final conditions, the final time τ is chosen to be large enough so as to correspond to a no-windshear condition. At the final time, four types of boundary conditions (BC0, BC1, BC2, BC3) are considered.

Boundary Condition BC0. Here, all of the state variables are free at the final point.

Boundary Condition BC1. Here,

$$\gamma(\tau)=\gamma_0. \tag{21}$$

The remaining state variables are free at the final point.

Boundary Conditions BC2. Here,

$$V(\tau)=V_0, \qquad \gamma(\tau)=\gamma_0. \tag{22}$$

The remaining state variables are free at the final point.

Boundary Condition BC3. Here,

$$V(\tau)=V_0, \qquad \gamma(\tau)=\gamma_0, \tag{23a}$$

$$\alpha(\tau)=\alpha_0. \tag{23b}$$

The remaining state variables are free at the final point. Upon combining (15) and (23b), we see that the specification of the final value of α implies the specification of the final value of u, that is,

$$u(\tau) = u_0 = \sqrt{(\alpha_* - \alpha_0)}. \tag{23c}$$

Comment. Use of (21) means that, at the final point, one intends to restore the initial value of the path inclination. Use of (22) means that, at the final point, one intends to restore the initial values of both the velocity and the path inclination. Finally, use of (23) means that, at the final point, one intends to restore the initial values of the velocity, the path inclination, and the angle of attack; hence, if the initial values (20) correspond to quasi-steady flight, then the final values (23) also correspond to quasi-steady flight.

8. Optimal Control Problems for Take-Off Trajectories

We refer to the system described in Sections 3–7. We assume that the wind flow field is known in advance. We assume that the power setting is given, so that the only control is the angle of attack, treated here as a state variable. In addition, we assume that the initial conditions (20) are given in conjunction with one of the final conditions BC0, BC1, BC2, BC3. With this understanding and with particular reference to take-off trajectories, we formulate the following optimization problems.

Problem (P1). Minimize the time integral of the difference squared between the flight altitude and a reference value, assumed to be a linear function of the horizontal distance. In this problem, the performance index is given by

$$I = \int_0^\tau (h - h_R)^2 \, dt, \tag{24a}$$

where

$$h_R = h_0 + K(x - x_0), \qquad K = \tan \gamma_{e0}. \tag{24b}$$

This is a Bolza problem of optimal control.

Problem (P2). Minimize the time integral of the difference squared between the relative path inclination and a reference value, assumed constant. In this problem, the performance index is given by

$$I = \int_0^\tau (\gamma - \gamma_R)^2 \, dt, \tag{25a}$$

where

$$\gamma_R = \gamma_0. \tag{25b}$$

This is a Bolza problem of optimal control.

Problem (P3). Minimize the time integral of the difference squared between the absolute path inclination and a reference value, assumed constant. In this problem, the performance index is given by

$$I = \int_0^\tau (\gamma_e - \gamma_{eR})^2 \, dt, \tag{26a}$$

where

$$\gamma_{eR} = \gamma_{e0}. \tag{26b}$$

This is a Bolza problem of optimal control.

Problem (P4). Minimize the peak value of the difference between a reference altititude, assumed constant, and the flight altitude. In this problem, the performance index is given by

$$I = \max_t (h_R - h), \qquad 0 \leq t \leq \tau, \tag{27a}$$

where h_R is a constant, to be specified in such a way that the difference $h_R - h$ is positive at all time instants. This is a minimax problem or Chebyshev problem of optimal control. It can be reformulated as a Bolza problem of optimal control (Ref. 37), in which one minimizes the integral performance index

$$J = \int_0^\tau (h_R - h)^q \, dt, \tag{27b}$$

for large values of the positive exponent q. This problem is of interest if the aircraft undershoots the initial altitude.

Problem (P5). Minimize the peak value of the weighted difference between a reference altitude, assumed constant, and the flight altitude; here, h_R is chosen as in Problem (P4) and the positive weighting function $G(t)$ or $G(h)$ is chosen so as to deemphasize the importance of the initial portion of the trajectory. In this problem, the performance index is given by

$$I = \max_t [G(h_R - h)], \qquad 0 \leq t \leq \tau. \tag{28a}$$

This is a minimax problem or Chebyshev problem of optimal control. It can be reformulated as a Bolza problem of optimal control (Ref. 37), in which one minimizes the integral performance index

$$J=\int_0^\tau [G(h_R-h)]^q\,dt, \tag{28b}$$

for large values of the positive exponent q. This problem is of interest if the aircraft does not undershoot the initial altitude.

Problem (P6). Minimize the peak value of the modulus of the difference between the flight altitude and a reference value, assumed to be a linear function of the horizontal distance, as in Problem (P1). In this problem, the performance index is given by

$$I=\max_t|h-h_R|, \qquad 0\leq t\leq\tau, \tag{29a}$$

where

$$h_R=h_0+K(x-x_0), \qquad K=\tan\gamma_{e0}. \tag{29b}$$

This is a minimax problem or Chebyshev problem of optimal control. It can be reformulated as a Bolza problem of optimal control (Ref. 37), in which one minimizes the integral performance index

$$J=\int_0^\tau (h-h_R)^q\,dt, \tag{29c}$$

for large values of the positive, even exponent q. This problem is of interest if the aircraft does not undershoot the initial altitude.

Problem (P7). Minimize the peak value of the modulus of the difference between the relative path inclination and a reference value, assumed constant, as in Problem (P2). In this problem, the performance index is given by

$$I=\max_t|\gamma-\gamma_R|, \qquad 0\leq t\leq\tau, \tag{30a}$$

where

$$\gamma_R=\gamma_0. \tag{30b}$$

This is a minimax problem or Chebyshev problem of optimal control. It can be reformulated as a Bolza problem of optimal control (Ref. 37), in which one minimizes the integral performance index

$$J=\int_0^\tau (\gamma-\gamma_R)^q\,dt, \tag{30c}$$

for large values of the positive, even exponent q.

Problem (P8). Minimize the peak value of the modulus of the difference between the absolute path inclination and a reference value; here, the reference value is assumed to be constant, as in Problem (P3). In this problem, the performance index is given by

$$I = \max_t |\gamma_e - \gamma_{eR}|, \qquad 0 \leq t \leq \tau, \tag{31a}$$

where

$$\gamma_{eR} = \gamma_{e0}. \tag{31b}$$

This is a minimax problem or Chebyshev problem of optimal control. It can be reformulated as a Bolza problem of optimal control (Ref. 37), in which one minimizes the integral performance index

$$J = \int_0^\tau (\gamma_e - \gamma_{eR})^q \, dt, \tag{31c}$$

for large values of the positive, even exponent q.

9. Sequential Gradient-Restoration Algorithm

In the previous section, we formulated eight problems of optimal control, the least-square problems (P1)-(P3) and the minimax problems (P4)-(P8). Problems (P1)-(P3) are Bolza problems, while Problems (P4)-(P8) are Chebyshev problems. By using a well-known theorem of functional analysis (Ref. 37), the Chebyshev problems were converted into Bolza problems. As a result, Problems (P1)-(P8) can all be treated as Bolza problems of optimal control.

Problems (P1)-(P8) can be solved using the family of sequential gradient-restoration algorithms for optimal control problems (SGRA, Refs. 18-24), in either the primal formulation (PSGRA, Refs. 18-22) or the dual formulation (DSGRA, Refs. 23-24). Regardless of whether the primal formulation is used or the dual formulation is used, sequential gradient-restoration algorithms involve a sequence of two-phase cycles, each cycle including a gradient phase and a restoration phase. In the gradient phase, the value of the augmented functional is decreased, while avoiding excessive constraint violation. In the restoration phase, the value of the constraint error is decreased, while avoiding excessive change in the value of the functional. In a complete gradient-restoration cycle, the value of the functional is decreased, while the constraints are satisfied to a preselected degree of accuracy. Thus, a succession of suboptimal solutions is generated, each new solution being an improvement over the previous one from the point of view of the value of the functional being minimized.

The convergence conditions are represented by the relations

$$P \leq \varepsilon_1, \qquad Q \leq \varepsilon_2. \tag{32}$$

Here, P is the norm squared of the error in the constraints, Q is the norm squared of the error in the optimality conditions, and ε_1, ε_2 are preselected, small, positive numbers.

In this work, the sequential gradient-restoration algorithm was employed in conjunction with the dual formulation. The algorithmic details can be found in Ref. 3. They are omitted here, for the sake of brevity.

10. Data for the Examples

In this section, we present the data used in the numerical experiments. The airplane under consideration is a Boeing B-727 aircraft with three JT8D-17 turbofan engines. It is assumed that the aircraft has become airborne from a runway located at sea-level altitude. It is also assumed that the ambient temperature is 100 deg Fahrenheit.

Thrust. It is assumed that the engines are operating at maximum power setting. The dependence of the thrust on the altitude is disregarded, and the thrust is assumed to depend on the velocity only. At $h = 0$ ft, the thrust is represented by Eq. (4), with

$$A_0 = \ 0.4456E+05 \text{ lb}, \qquad 0 \leq V \leq 422 \text{ ft sec}^{-1}, \tag{33a}$$

$$A_1 = -0.2398E+02 \text{ lb ft}^{-1} \text{ sec}, \qquad 0 \leq V \leq 422 \text{ ft sec}^{-1}, \tag{33b}$$

$$A_2 = \ 0.1442E-01 \text{ lb ft}^{-2} \text{ sec}^2, \qquad 0 \leq V \leq 422 \text{ ft sec}^{-1}. \tag{33c}$$

The inclination of the thrust with respect to the aircraft reference line is assumed to be

$$\delta = 0.2000E+01 \text{ deg}. \tag{34}$$

Drag. The dependence of the density on the altitude is disregarded, and the drag is assumed to depend on the velocity and the angle of attack only. This function is represented by Eqs. (5)-(6), with[7]

$$\rho = 0.2203E-02 \text{ lb ft}^{-4} \text{ sec}^2, \tag{35a}$$

$$S = 0.1560E+04 \text{ ft}^2, \tag{35b}$$

[7] The aerodynamic data refer to gear up and flap setting $\delta_F = 15$ deg.

and

$$B_0 = \ 0.7351E-01, \qquad 0 \le \alpha \le 16 \text{ deg}, \tag{36a}$$

$$B_1 = -0.8617E-01, \qquad 0 \le \alpha \le 16 \text{ deg}, \tag{36b}$$

$$B_2 = \ 0.1996E+01, \qquad 0 \le \alpha \le 16 \text{ deg}. \tag{36c}$$

Lift. Like the drag, the lift is assumed to depend on the velocity and the angle of attack only. This function is represented by Eqs. (7)-(8), with ρ, S given by Eqs. (35) and

$$C_0 = \ 0.1667E+00, \qquad 0 \le \alpha \le 16 \text{ deg}, \tag{37a}$$

$$C_1 = \ 0.6231E+01, \qquad 0 \le \alpha \le 16 \text{ deg}, \tag{37b}$$

$$C_2 = -0.2165E+02, \qquad 12 \le \alpha \le 16 \text{ deg}. \tag{37c}$$

Weight. The weight of the aircraft is assumed to be constant, specifically,

$$W = 0.1800E+06 \text{ lb}. \tag{38}$$

Windshear. The wind model is governed by Eqs. (10), with[8]

$$W_x = -k, \qquad x \le a, \tag{39a}$$

$$W_x = -k+2k(x-a)/(b-a), \qquad a \le x \le b, \tag{39b}$$

$$W_x = \ k, \qquad x \ge b. \tag{39c}$$

Therefore, the wind velocity difference is

$$\Delta W_x = 2k \tag{40a}$$

and the windshear intensity is

$$\Delta W_x/\Delta x = 2k/(b-a). \tag{40b}$$

In windshear model WS1, the constants a, b are given by

$$a = 0.3000E+03 \text{ ft}, \qquad b = 0.4300E+04 \text{ ft}. \tag{41a}$$

In windshear model WS2, the constants a, b are given by

$$a = 0.1000E+04 \text{ ft}, \qquad b = 0.5000E+04 \text{ ft}. \tag{41b}$$

In windshear model WS3, the constants a, b are given by

$$a = 0.2000E+04 \text{ ft}, \qquad b = 0.6000E+04 \text{ ft}. \tag{41c}$$

[8] The wind model involves corners, which are smoothed using the technique discussed in Section 5. Each smoothing interval is assumed to be 600 ft in length and is centered around the respective corner.

With the constants a, b known, Eqs. (39)-(40) represent a one-parameter family of wind models. The parameter k determines both the wind velocity difference (40a) and the windshear intensity (40b). Table 1 shows the values of ΔW_x and $\Delta W_x/\Delta x$ for several values of the parameter k. Small values of k correspond to windshears that are survivable, while large values of k correspond to windshears that are not survivable.

Inequality Constraints. The angle of attack is subject to Ineq. (14), with

$$\alpha_* = 0.1600E+02 \text{ deg}. \tag{42}$$

The time derivative of the angle of attack is subject to the Ineq. (16), with

$$C = 0.3000E+01 \text{ deg sec}^{-1}. \tag{43}$$

The constant ε in Eqs. (17)-(18) is set at the level

$$\varepsilon = 0.4000E+00. \tag{44}$$

Initial Conditions. The following initial conditions are assumed:

$$x(0) = 0.0000E+00 \text{ ft}, \tag{45a}$$

$$h(0) = 0.5000E+02 \text{ ft}, \tag{45b}$$

$$V(0) = 0.2768E+03 \text{ ft sec}^{-1}, \tag{45c}$$

$$\gamma(0) = 0.6989E+01 \text{ deg}, \tag{45d}$$

$$\alpha(0) = 0.1036E+02 \text{ deg}. \tag{45e}$$

Table 1. Wind velocity difference and windshear intensity.

k (ft sec^{-1})	ΔW_x (ft sec^{-1})	$\Delta W_x/\Delta x$ (sec^{-1})
10	20	0.005
20	40	0.010
30	60	0.015
40	80	0.020
50	100	0.025
60	120	0.030
70	140	0.035
80	160	0.040
90	180	0.045
100	200	0.050

Final Time. The final time is set at the value

$$\tau = 0.4000E+02 \text{ sec.} \tag{46}$$

Final Conditions. Four types of final conditions are considered.

In boundary condition model BC0, all of the state variables are free at the final point.

In boundary condition model BC1, it is required that

$$\gamma(\tau) = 0.6989E+01 \text{ deg.} \tag{47}$$

In boundary condition model BC2, it is required that

$$V(\tau) = 0.2768E+03 \text{ ft sec}^{-1}, \tag{48a}$$

$$\gamma(\tau) = 0.6989E+01 \text{ deg.} \tag{48b}$$

In boundary condition model BC3, it is required that

$$V(\tau) = 0.2768E+03 \text{ ft sec}^{-1}, \tag{49a}$$

$$\gamma(\tau) = 0.6989E+01 \text{ deg}, \tag{49b}$$

$$\alpha(\tau) = 0.1036E+02 \text{ deg.} \tag{49c}$$

Note that the initial conditions (45) correspond to quasi-steady flight and that the final conditions (49) also correspond to quasi-steady flight. Therefore, use of (45) in combination with (49) implies that an optimal transition from quasi-steady flight to quasi-steady flight is desired.

Performance Indexes. The numerical constants appearing in the performance indexes of Section 8 are given below.

For the least-square problems [Problems (P1)-(P3)], the constants appearing in Eqs. (24)-(26) are given by

(P1) $$x_0 = 0.0000E+00 \text{ ft}, \tag{50a}$$

$$h_0 = 0.5000E+02 \text{ ft}, \tag{50b}$$

$$\gamma_{e0} = 0.8165E+01 \text{ deg}, \tag{50c}$$

$$K = 0.1435E+00; \tag{50d}$$

(P2) $$\gamma_R = 0.6989E+01 \text{ deg}; \tag{51}$$

(P3) $$\gamma_{eR} = 0.8165E+01 \text{ deg.} \tag{52}$$

For the minimax problems [Problems (P4)-(P8)], the constants appearing in Eqs. (27)-(31) are given by

$$\text{(P4)} \quad h_R = 0.9000E+03 \text{ ft}; \tag{53}$$

$$\text{(P5)} \quad h_R = 0.9000E+03 \text{ ft}; \tag{54}$$

$$\text{(P6)} \quad x_0 = 0.0000E+00 \text{ ft}, \tag{55a}$$

$$h_0 = 0.5000E+02 \text{ ft}, \tag{55b}$$

$$\gamma_{e0} = 0.8165E+01 \text{ deg}, \tag{55c}$$

$$K = 0.1435E+00; \tag{55d}$$

$$\text{(P7)} \quad \gamma_R = 0.6989E+01 \text{ deg}; \tag{56}$$

$$\text{(P8)} \quad \gamma_{eR} = 0.8165E+01 \text{ deg}. \tag{57}$$

For the minimax problems [Problems (P4) and (P6)-(P8)], the exponent q was set at the level

$$q = 6. \tag{58}$$

For the weighted minimax problem [Problem (P5)], the exponent q was set at the level

$$q = 2, \tag{59}$$

and the weighting function $G(t)$ was specified to be

$$G(t) = \exp[-20(t/40-0.8)^2]. \tag{60}$$

Remark. The velocity appearing in the initial conditions (45) is FAA certification velocity V_2, augmented by 10 knots. In turn, the velocity V_2+10 (in knots) corresponds approximately to the steepest climb condition in quasi-steady flight.

11. Numerical Results

Problems (P1)-(P8) were solved employing the sequential gradient-restoration algorithm in connection with the dual formulation (DSGRA, Refs. 23-24). This algorithm was programmed in FORTRAN IV, and the numerical results were obtained in double-precision arithmetic. Computations were performed at Rice University using an NAS-AS-9000 computer.

The interval of integration was divided into 100 steps. The differential systems were integrated using Hamming's modified predictor-corrector method, with a special Runge-Kutta starting procedure. Definite integrals were computed using a modified Simpson's rule. Linear algebraic systems were solved using a standard Gaussian elimination routine.

A large number of combinations of performance indexes, windshear models, windshear intensities, and boundary conditions was considered (see Refs. 1–5). Here, for the sake of brevity, we restrict the presentation to Problems (P6), (P7) and windshear model WS1. For the remaining problems, see Ref. 4.

For computational efficiency, the state variables and the time were scaled by employing the following reference values:

$$\tilde{x} = 1000 \text{ ft}, \tag{61a}$$

$$\tilde{h} = 1000 \text{ ft}, \tag{61b}$$

$$\tilde{V} = 1000 \text{ ft sec}^{-1}, \tag{61c}$$

$$\tilde{\gamma} = 57.30 \text{ deg}, \tag{61d}$$

$$\tilde{t} = 40 \text{ sec}. \tag{61e}$$

For each problem, the functional being minimized was suitably scaled. The following stopping conditions were employed for the dual sequential gradient-restoration algorithm:

$$P \leq E - 10, \qquad Q \leq E - 08, \tag{62}$$

where P denotes the constraint error and Q denotes the error in the optimality conditions.

The results are given in Figs. 5–10. Each figure contains six parts: the wind velocity W_x; the flight altitude h; the relative velocity V; the relative path inclination γ; the angle of attack α; the lift-to-weight ratio L/W, the thrust-to-weight ratio T/W, the drag-to-weight ratio D/W, and the windshear inertia force-to-weight ratio W_F/W.

Case 1. Problem (P6); minimax $|\Delta h|$; boundary condition model BC3; windshear model WS1; wind velocity difference $\Delta W_x = 80 \text{ ft sec}^{-1}$; windshear intensity $\Delta W_x/\Delta x = 0.020 \text{ sec}^{-1}$.

This is a particularly difficult problem, because it implies a transition from quasi-steady flight to quasi-steady flight. The optimal trajectory is shown in Fig. 5 together with two comparison trajectories, namely, the constant-angle-of-attack trajectory $\alpha = \alpha_0 = 10.36$ deg and the constant-angle-of-attack trajectory $\alpha = \alpha_* = 16$ deg.

Figure 5B shows that the optimal trajectory is considerably superior to the constant-angle-of-attack trajectories in terms of avoidance of the ground. Indeed, the trajectory $\alpha = \alpha_0$ hits the ground, while the trajectory $\alpha = \alpha_*$ comes close to the ground.

Figures 5C and 5D show that, by comparison with the constant-angle-of-attack trajectories, the optimal trajectory is characterized by smaller excursions in both the velocity and the path inclination. It is interesting to

observe that the optimal trajectory achieves the minimum velocity at about the time when the windshear vanishes; on the other hand, the constant-angle-of-attack trajectories achieve the minimum velocity at earlier times.

Figure 5E shows that a large portion of the optimal trajectory is flown at an angle of attack below the maximum value $\alpha_* = 16$ deg. However, for a brief time interval (about 3 sec), the maximum value of α is reached.

Figure 5F shows that the windshear inertia force is larger than the drag over a considerable time interval (15 sec). In this time interval, the sum of the windshear inertia force and the drag exceeds the thrust of the aircraft, even though maximum power setting is employed. This explains why, even for a moderately severe windshear, the optimal trajectory exhibits a considerable deviation from the ideal trajectory flown under no windshear conditions.

Case 2. Problem (P7); minimax $|\Delta\gamma|$; boundary condition model BC3; windshear model WS1; wind velocity difference $\Delta W_x = 80$ ft sec^{-1}; windshear intensity $\Delta W_x/\Delta x = 0.020$ sec^{-1}.

Case 2 differs from Case 1, because the performance index being minimaximized is $|\Delta\gamma|$, instead of $|\Delta h|$. The optimal trajectory is shown in Fig. 6.

Upon comparing Figs. 5 and 6, we see a similarity of behavior, with two exceptions: (i) the altitude distribution for Case 2 exhibits a monotonic behavior (Fig. 6B), while the altitude distribution for Case 1 exhibits a dip before final climbing is resumed (Fig. 5B); and (ii) the angle-of-attack distribution for Case 2 is well below the maximum value $\alpha_* = 16$ deg, while the angle-of-attack distribution for Case 1 attains the maximum value. Because of (i) and (ii), we conclude that the trajectory minimaximizing $|\Delta\gamma|$ is to be preferred to the trajectory minimaximizing $|\Delta h|$.

Case 3. Problem (P6); minimax $|\Delta h|$; boundary condition model BC3; windshear model WS1; wind velocity difference $\Delta W_x = 100$ ft sec^{-1}; windshear intensity $\Delta W_x/\Delta x = 0.025$ sec^{-1}.

Case 3 differs from Case 1, because the wind velocity difference has been increased from 80 to 100 ft sec^{-1} and the windshear intensity has been increased from 0.020 to 0.025 sec^{-1}. The optimal trajectory is shown in Fig. 7.

Upon comparing Figs. 5 and 7, we see that a similarity of behavior exists. The following points must be noted: (i) the final altitude for Case 3 is below the final altitude for Case 1; (ii) the time interval over which maximum angle of attack is needed increases from 3 sec in Case 1 to 8 sec in Case 3; (iii) to fly optimally in Case 3 is more critical than to fly optimally

in Case 1; this is due to the fact that, in Case 3, both the trajectory $\alpha = \alpha_0$ and the trajectory $\alpha = \alpha_*$ hit the ground.

Case 4. Problem (P7); minimax $|\Delta\gamma|$; boundary condition model BC3; windshear model WS1; wind velocity difference $\Delta W_x = 100$ ft sec^{-1}; windshear intensity $\Delta W_x/\Delta x = 0.025$ sec^{-1}.

Case 4 differs from Case 2, because the wind velocity difference has been increased from 80 to 100 ft sec^{-1} and the windshear intensity has been increased from 0.020 to 0.025 sec^{-1}. The optimal trajectory is shown in Fig. 8.

Upon comparing Figs. 6 and 8, we see that a similarity of behavior exists. The following points must be noted: (i) the final altitude for Case 4 is below the final altitude for Case 2; however, the monotonic behavior of the altitude distribution is retained; (ii) the angle of attack distribution for Case 4 is below the maximum value $\alpha_* = 16$ deg; however, the peak value of α in Case 4 is higher than the peak value of α in Case 2.

If one compares Case 4 (Fig. 8) with Case 3 (Fig. 7), one concludes once more that the trajectory minimaximizing $|\Delta\gamma|$ is to be preferred to the trajectory minimaximizing $|\Delta h|$.

Case 5. Problem (P7); minimax $|\Delta\gamma|$; boundary condition models BC0, BC1, BC2, BC3; windshear model WS1; wind velocity difference $\Delta W_x = 80$ ft sec^{-1}; windshear intensity $\Delta W_x/\Delta x = 0.020$ sec^{-1}.

In Cases 1–4, only one type of boundary condition was considered, namely, model BC3. In Case 5, we consider four types of boundary conditions, namely, models BC0, BC1, BC2, BC3. In model BC0, the final values of the state variables are all free; in model BC1, the final value of γ is given; in model BC2, the final values of V, γ are given; in model BC3, the final values of V, γ, α are given. While model BC3 implies a transition from quasi-steady flight to quasi-steady flight, this is not the case with models BC0, BC1, BC2. The optimal trajectories for boundary condition models BC0, BC1, BC2, BC3 are shown in Fig. 9.

Upon inspecting Fig. 9, we see that a similarity of behavior exists between the optimal trajectories associated with models BC0, BC1, BC2, BC3. The following points must be noted: (i) the altitude distribution exhibits a monotonic behavior, regardless of the boundary condition model employed; (ii) the optimal trajectories for models BC0, BC1 are quite close to one another; an analogous remark holds for the optimal trajectories for models BC2, BC3; (iii) the optimal trajectories for models BC0, BC1 achieve a higher final altitude than the optimal trajectories for models BC2, BC3; however, the higher final altitude is obtained at the expense of a considerable

velocity loss; (iv) the optimal trajectories for models BC0, BC1 are characterized by higher values of the angle of attack than the optimal trajectories for models BC2, BC3.

Case 6. Problem (P7); minimax $|\Delta\gamma|$; boundary condition model BC1; windshear model WS1; wind velocity differences $\Delta W_x = 80$, 100, 120, 140 ft sec^{-1}; windshear intensities $\Delta W_x/\Delta x = 0.020, 0.025, 0.030, 0.035$ sec^{-1}.

In Case 6, we consider the effect of different wind velocity differences, and hence different windshear intensities, on trajectories minimaximizing $|\Delta\gamma|$ in conjunction with boundary condition model BC1. The optimal trajectories for wind velocity differences $\Delta W_x = 80$, 100, 120, 140 ft sec^{-1} are shown in Fig. 10.

Upon inspecting Fig. 10, the following points must be noted: (i) as the wind velocity difference increases, the altitude distribution exhibits considerable change, while this is not the case with the velocity distribution and the angle of attack distribution; (ii) if the wind velocity difference is $\Delta W_x = 80$ ft sec^{-1} or $\Delta W_x = 100$ ft sec^{-1}, the altitude distribution has a monotonically climbing behavior; if the wind velocity difference is increased to $\Delta W_x = 120$ ft sec^{-1}, the altitude distribution is characterized by a dip; if the wind velocity difference is further increased to $\Delta W_x = 140$ ft sec^{-1}, the altitude distribution is characterized by a major dip, so that the optimal trajectory hits the ground; (iii) with reference to the case $\Delta W_x = 140$ ft sec^{-1}, Fig. 10F shows that the windshear inertia force is larger than both the drag and the thrust over a considerable time interval (14 sec); this explains why the optimal trajectory hits the ground.

12. Conclusions

This paper is concerned with optimal flight trajectories in the presence of windshear. With particular reference to take-off, eight fundamental optimization problems [Problems (P1)-(P8)] are formulated under the assumptions that the power setting is held at the maximum value and that the airplane is controlled through the angle of attack.

Problems (P1)-(P3) are least-square problems of the Bolza type. Problems (P4)-(P8) are minimax problems of the Chebyshev type, which can be converted into Bolza problems through suitable transformations. These problems are solved employing the dual sequential gradient-restoration algorithm (DSGRA) for optimal control problems.

Numerical results are obtained for a large number of combinations of performance indexes, boundary conditions, windshear models, and windshear intensities. However, for the sake of brevity, the presentation of this paper is restricted to Problem (P6), minimax $|\Delta h|$, and Problem (P7),

minimax $|\Delta\gamma|$. Inequality constraints are imposed on the angle of attack and the time derivative of the angle of attack. The following conclusions are reached:

(i) optimal trajectories are considerably superior to constant-angle-of-attack trajectories;

(ii) optimal trajectories achieve minimum velocity at about the time when the windshear ends;

(iii) optimal trajectories can be found which transfer an aircraft from a quasi-steady condition to a quasi-steady condition through a windshear;

(iv) as the boundary conditions are relaxed, a higher final altitude can be achieved, albeit at the expense of a considerable velocity loss;

(v) among the optimal trajectories investigated, those solving Problem (P7) are to be preferred, because the altitude distribution exhibits a monotonic behavior; in addition, for boundary conditions BC2 and BC3, the peak angle of attack is below the maximum permissible value;

(vi) moderate windshears and relatively severe windshears are survivable employing an optimized flight strategy; however, extremely severe windshears are not survivable, even employing an optimized flight strategy;

(vii) the sequential gradient-restoration algorithm (SGRA), employed in its dual form (DSGRA), has proven to be a powerful algorithm for solving the problem of the optimal flight trajectories in a windshear.

In subsequent papers, the analysis presented here for optimal take-off trajectories will be extended to include (i) rotational motion effects, (ii) a more complete windshear model, and (iii) guidance laws. In particular, for guidance strategies for near-optimum take-off performance in a windshear, see Ref. 38. Also in subsequent papers, the treatment developed for optimal take-off trajectories will be extended to include optimal landing trajectories.

References

1. MIELE, A., WANG, T., and MELVIN, W. W., *Optimal Flight Trajectories in the Presence of Windshear, Part 1, Equations of Motion*, Rice University, Aero-Astronautics Report No. 191, 1985.
2. MIELE, A., WANG, T., and MELVIN, W. W., *Optimal Flight Trajectories in the Presence of Windshear, Part 2, Problem Formulation, Take-Off*, Rice University, Aero-Astronautics Report No. 192, 1985.
3. MIELE, A., WANG, T., and MELVIN, W. W., *Optimal Flight Trajectories in the Presence of Windshear, Part 3, Algorithms*, Rice University, Aero-Astronautics Report No. 193, 1985.
4. MIELE, A., WANG, T., and MELVIN, W. W., *Optimal Flight Trajectories in the Presence of Windshear, Part 4, Numerical Results, Take-Off*, Rice University, Aero-Astronautics Report No. 194, 1985.

5. MIELE, A., *Summary Report on NASA Grant No. NAG-1-516, Optimal Flight Trajectories in the Presence of Windshear, 1984–85*, Rice University, Aero-Astronautics Report No. 195, 1985.
6. ANONYMOUS, N. N., *Low Altitude Windshear and Its Hazard to Aviation*, National Academy Press, Washington, DC, 1983.
7. MIELE, A., *Flight Mechanics, Vol. 1, Theory of Flight Paths*, Addison-Wesley Publishing Company, Reading, Massachusetts, 1962.
8. FROST, W., and CROSBY, B., *Investigations of Simulated Aircraft Flight through Thunderstorm Outflows*, NASA, Contractor Report No. 3052, 1978.
9. MCCARTHY, J., BLICK, E. F., and BENSCH, R. R., *Jet Transport Performance in Thunderstorm Windshear Conditions*, NASA, Contractor Report No. 3207, 1979.
10. PSIAKI, M. L., and STENGEL, R. F., *Analysis of Aircraft Control Strategies for Microburst Encounter*, AIAA 22nd Aerospace Sciences Meeting, Reno, Nevada, Paper No. AIAA-84-0238, 1984.
11. FROST, W., and BOWLES, R. L., *Windshear Terms in the Equations of Aircraft Motion*, Journal of Aircraft, Vol. 21, No. 11, pp. 866–872, 1984.
12. ZHU, S. X., and ETKIN, B., *Fluid-Dynamic Model of a Downburst*, University of Toronto, Institute for Aerospace Studies, Report No. UTIAS-271, 1983.
13. ALEXANDER, M. B., and CAMP, D. W., *Wind Speed and Direction Shears with Associated Vertical Motion during Strong Surface Winds*, NASA, Technical Memorandum No. 82566, 1984.
14. FROST, W., CHANG, H. P., ELMORE, K. L., and MCCARTHY, J., *Simulated Flight through JAWS Windshear: In-Depth Analysis Results*, AIAA 22nd Aerospace Sciences Meeting, Reno, Nevada, Paper No. AIAA-84-0276, 1984.
15. CAMPBELL, C. W., *A Spatial Model of Windshear and Turbulence for Flight Simulation*, NASA, Technical Paper No. 2313, 1984.
16. ANONYMOUS, N. N., *Flight Path Control in Windshear*, Boeing Airliner, pp. 1–12, January–March, 1985.
17. LEITMANN, G., *The Calculus of Variations and Optimal Control*, Plenum Publishing Corporation, New York, New York, 1981.
18. MIELE, A., PRITCHARD, R. E., and DAMOULAKIS, J. N., *Sequential Gradient-Restoration Algorithm for Optimal Control Problems*, Journal of Optimization Theory and Applications, Vol. 5, No. 4, pp. 235–282, 1970.
19. MIELE, A., DAMOULAKIS, J. N., CLOUTIER, J. R., and TIETZE, J. L., *Sequential Gradient-Restoration Algorithm for Optimal Control Problems with Nondifferential Constraints*, Journal of Optimization Theory and Applications, Vol. 13, No. 2, pp. 218–255, 1974.
20. MIELE, A., *Recent Advances in Gradient Algorithms for Optimal Control Problems*, Journal of Optimization Theory and Applications, Vol. 17, Nos. 5/6, pp. 361–430, 1975.
21. GONZALEZ, S., and MIELE, A., *Sequential Gradient-Restoration Algorithm for Optimal Control Problems with General Boundary Conditions*, Journal of Optimization Theory and Applications, Vol. 26, No. 3, pp. 395–425, 1978.
22. MIELE, A., *Gradient Algorithms for the Optimization of Dynamic Systems*, Control and Dynamic Systems, Advances in Theory and Application, Edited by C. T. Leondes, Academic Press, New York, New York, Vol. 16, pp. 1–52, 1980.

23. MIELE, A., and WANG, T., *Primal-Dual Properties of Sequential Gradient-Restoration Algorithms for Optimal Control Problems, Part 1: Basic Problem*, Rice University, Aero-Astronautics Report No. 183, 1985.
24. MIELE, A., and WANG, T., *Primal-Dual Properties of Sequential Gradient-Restoration Algorithms for Optimal Control Problems, Part 2: General Problem*, Rice University, Aero-Astronautics Report No. 184, 1985.
25. JOHNSON, C. D., *Optimal Control with Chebyshev Minimax Performance Index*, Journal of Basic Engineering, Vol. 89, No. 2, pp. 251-262, 1967.
26. MICHAEL, G. J., *Computation of Chebyshev Optimal Control*, AIAA Journal, Vol. 9, No. 5, pp. 973-975, 1971.
27. WARGA, J., *Minimax Problems and Unilateral Curves in the Calculus of Variations*, SIAM Journal on Control, Vol. 3, No. 1, pp. 91-105, 1965.
28. POWERS, W. F., *A Chebyshev Minimax Technique Oriented to Aerospace Trajectory Optimization Problems*, AIAA Journal, Vol. 10, No. 10, pp. 1291-1296, 1972.
29. HOLMAKER, K., *A Minimax Optimal Control Problem*, Journal of Optimization Theory and Applications, Vol. 28, No. 3, pp. 391-410, 1979.
30. HOLMAKER, K., *A Property of an Autonomous Minimax Optimal Control Problem*, Journal of Optimization Theory and Applications, Vol. 32, No. 1, pp. 81-87, 1980.
31. MIELE, A., MOHANTY, B. P., VENKATARAMAN, P., and KUO, Y. M., *Numerical Solution of Minimax Problems of Optimal Control, Part 1*, Journal of Optimization Theory and Applications, Vol. 38, No. 1, pp. 97-109, 1982.
32. MIELE, A., MOHANTY, B. P., VENKATARAMAN, P., and KUO, Y. M., *Numerical Solution of Minimax Problems of Optimal Control, Part 2*, Journal of Optimization Theory and Applications, Vol. 38, No. 1, pp. 111-135, 1982.
33. MIELE, A., and VENKATARAMAN, P., *Optimal Trajectories for Aeroassisted Orbital Transfer*, Acta Astronautica, Vol. 11, Nos. 7/8, pp. 423-433, 1984.
34. MIELE, A., and VENKATARAMAN, P., *Minimax Optimal Control and Its Application to the Reentry of a Space Glider*, Recent Advances in the Aerospace Sciences, Edited by L. Casci, Plenum Publishing Corporation, New York, New York, pp. 21-40, 1985.
35. MIELE, A., and BASAPUR, V. K., *Approximate Solutions to Minimax Optimal Control Problems for Aeroassisted Orbital Transfer*, Acta Astronautica, Vol. 12, No. 10, pp. 809-818, 1985.
36. MIELE, A., BASAPUR, V. K., and MEASE, K. D., *Nearly-Grazing Optimal Trajectories for Aeroassisted Orbital Transfer*, Journal of the Astronautical Sciences, Vol. 34, No. 1, pp. 3-18, 1986.
37. MIELE, A., and WANG, T., *An Elementary Proof of a Functional Analysis Result Having Interest for Minimax Optimal Control of Aeroassisted Orbital Transfer Vehicles*, Rice University, Aero-Astronautics Report No. 182, 1985.
38. MIELE, A., WANG, T., and MELVIN, W. W., *Guidance Strategies for Near-Optimum Take-Off Performance in a Windshear*, Journal of Optimization Theory and Applications, Vol. 50, No. 1, pp. 1-35, 1986.

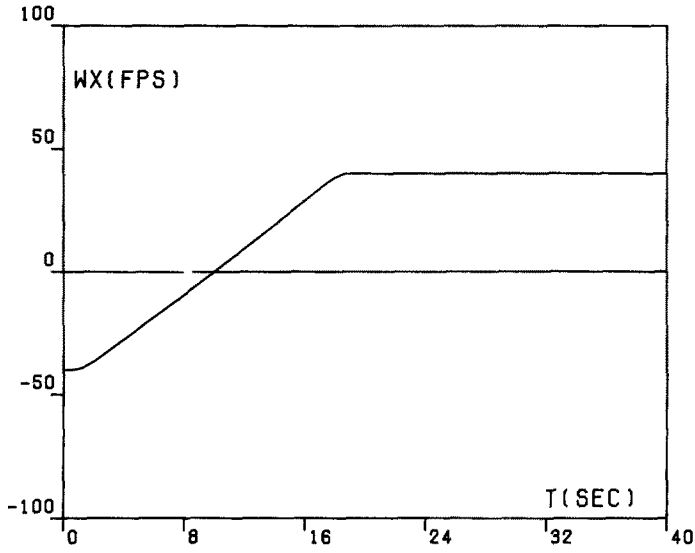

Fig. 5A. Horizontal component of the wind velocity W_x versus time t (Case 1).

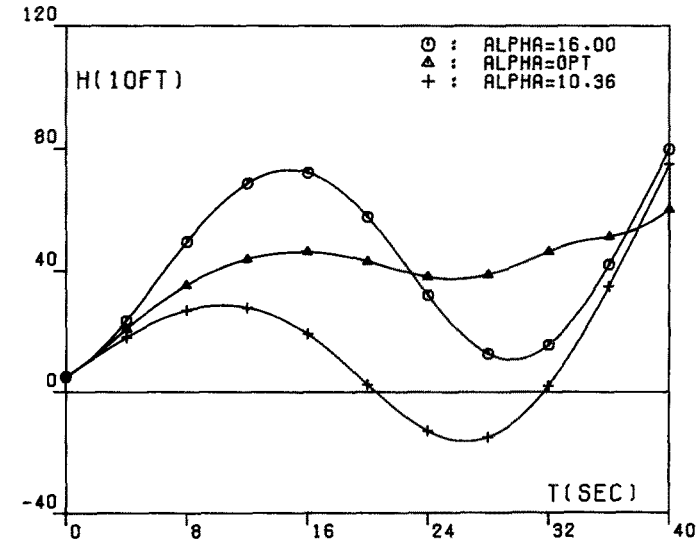

Fig. 5B. Altitude h versus time t (Case 1).

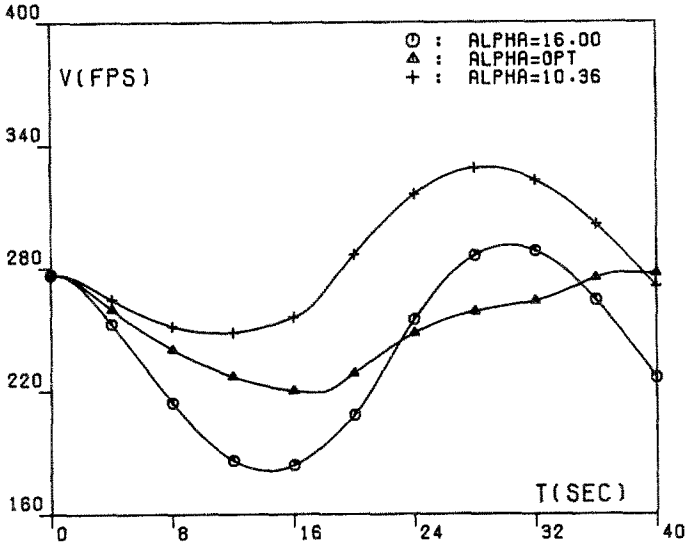

Fig. 5C. Relative velocity V versus time t (Case 1).

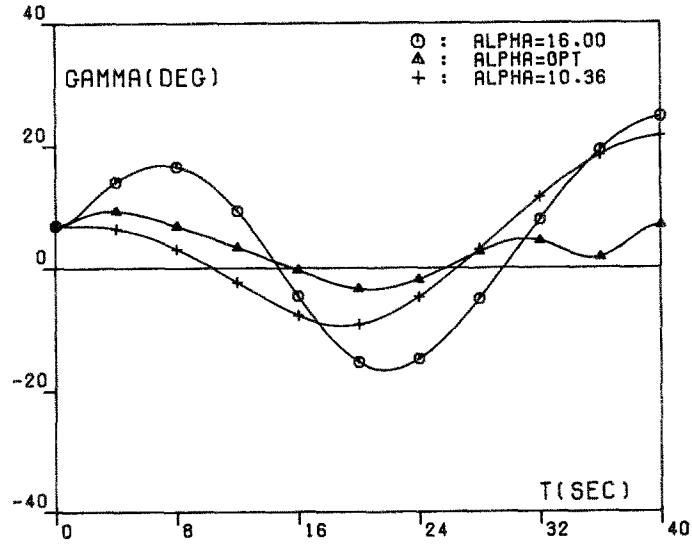

Fig. 5D. Relative path inclination γ versus time t (Case 1).

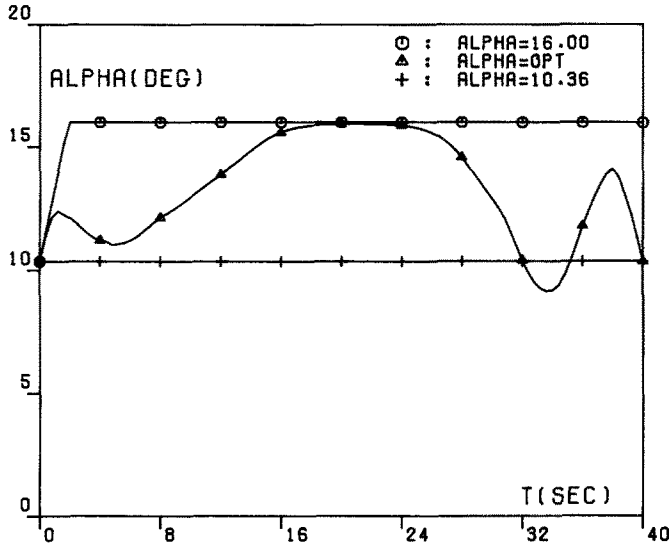

Fig. 5E. Relative angle of attack α versus time t (Case 1).

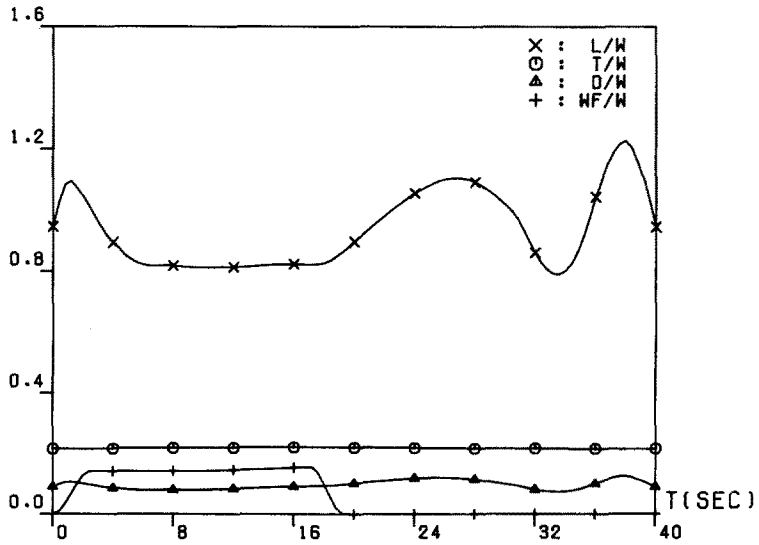

Fig. 5F. Lift-to-weight ratio L/W, thrust-to-weight ratio T/W, drag-to-weight ratio D/W, and windshear inertia force-to-weight ratio W_F/W versus time t (Case 1).

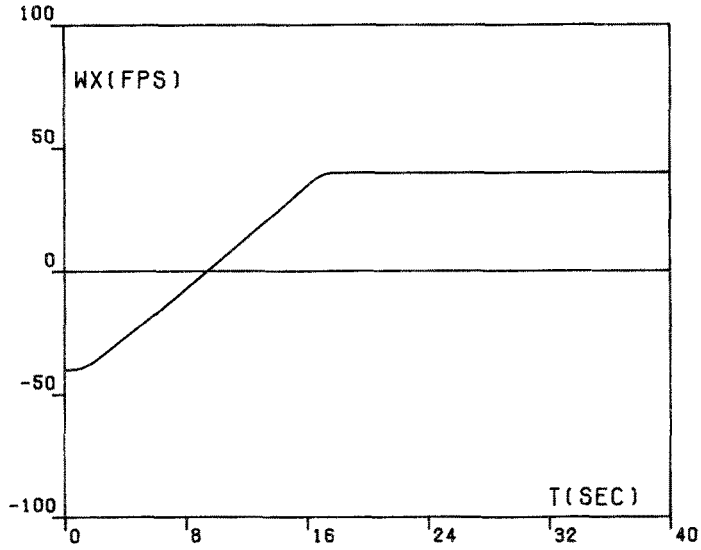

Fig. 6A. Horizontal component of the wind velocity W_x versus time t (Case 2).

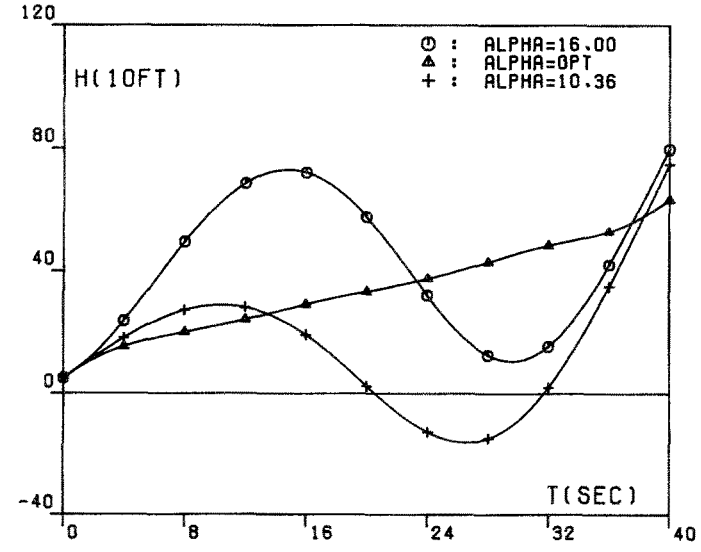

Fig. 6B. Altitude h versus time t (Case 2).

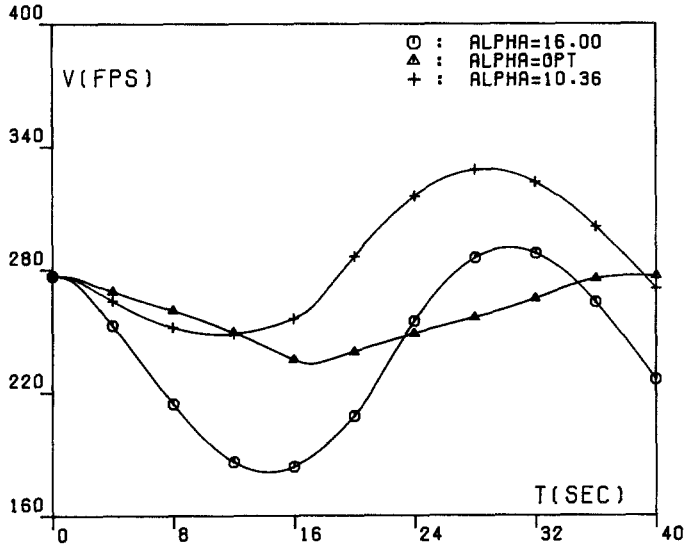

Fig. 6C. Relative velocity V versus time t (Case 2).

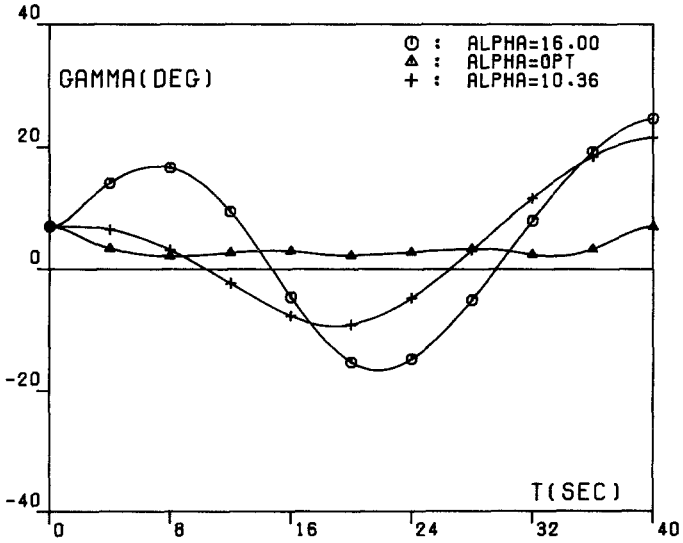

Fig. 6D. Relative path inclination γ versus time t (Case 2).

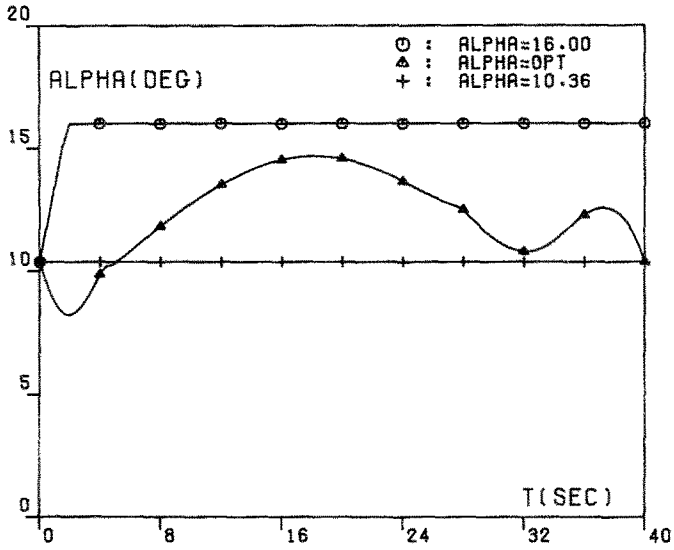

Fig. 6E. Relative angle of attack α versus time t (Case 2).

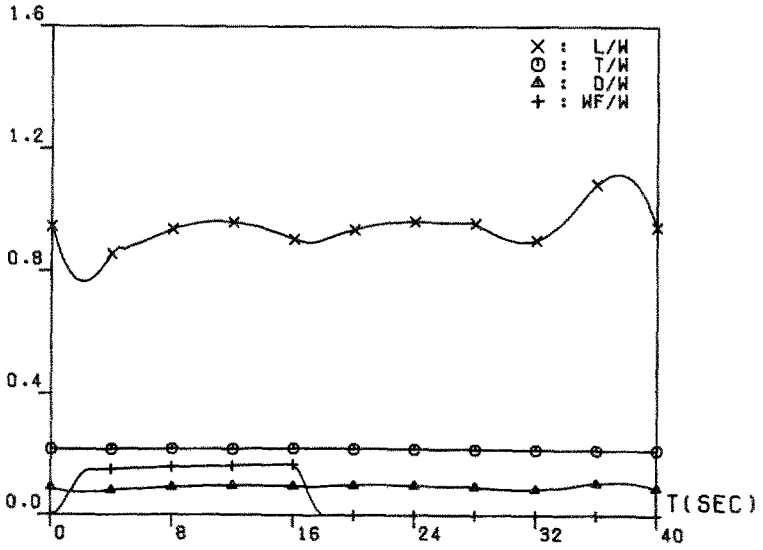

Fig. 6F. Lift-to-weight ratio L/W, thrust-to-weight ratio T/W, drag-to-weight ratio D/W, and windshear inertia force-to-weight ratio W_F/W versus time t (Case 2).

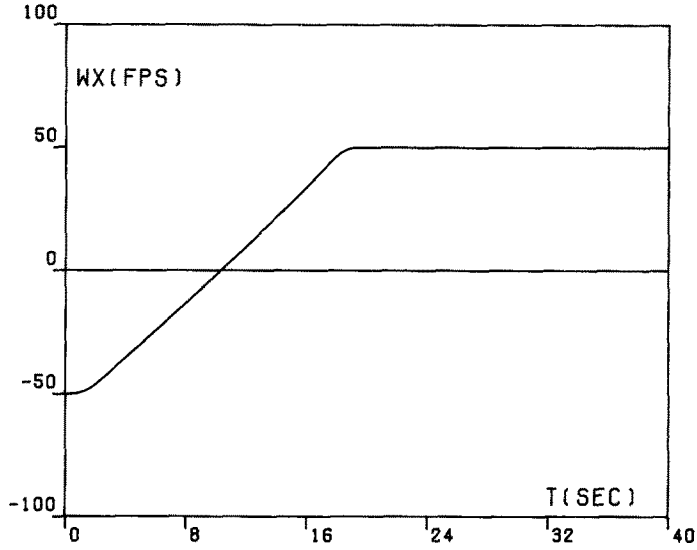

Fig. 7A. Horizontal component of the wind velocity W_x versus time t (Case 3).

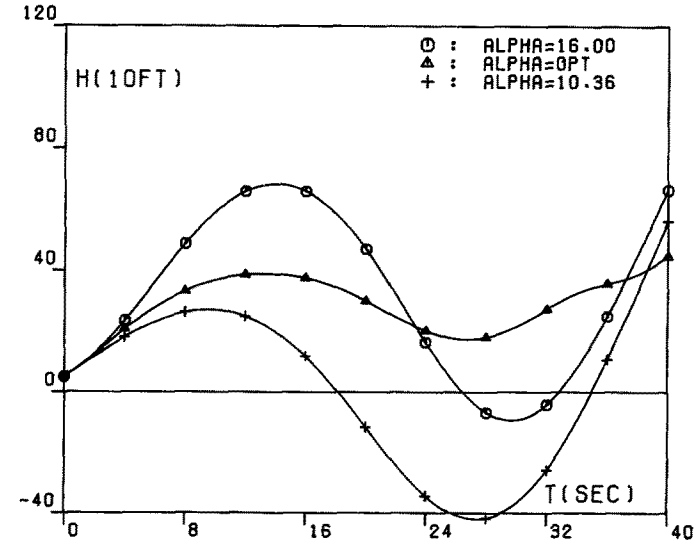

Fig. 7B. Altitude h versus time t (Case 3).

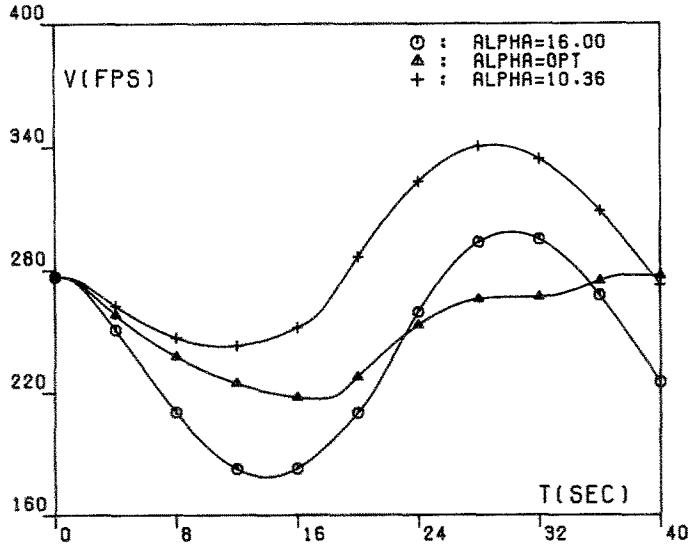

Fig. 7C. Relative velocity V versus time t (Case 3).

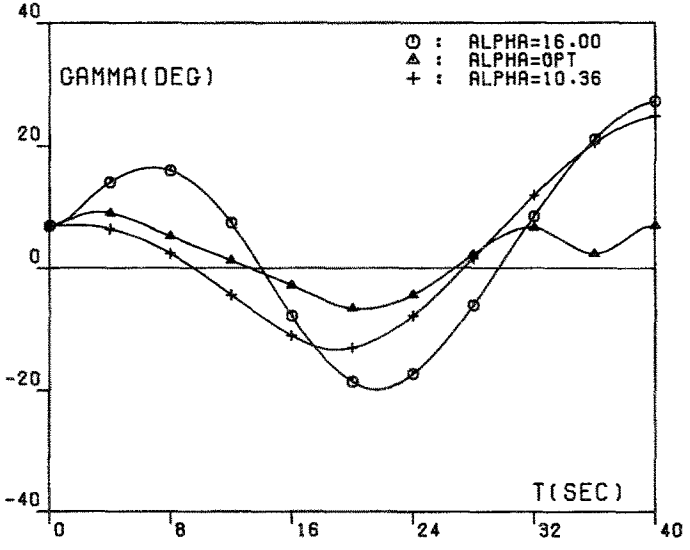

Fig. 7D. Relative path inclination γ versus time t (Case 3).

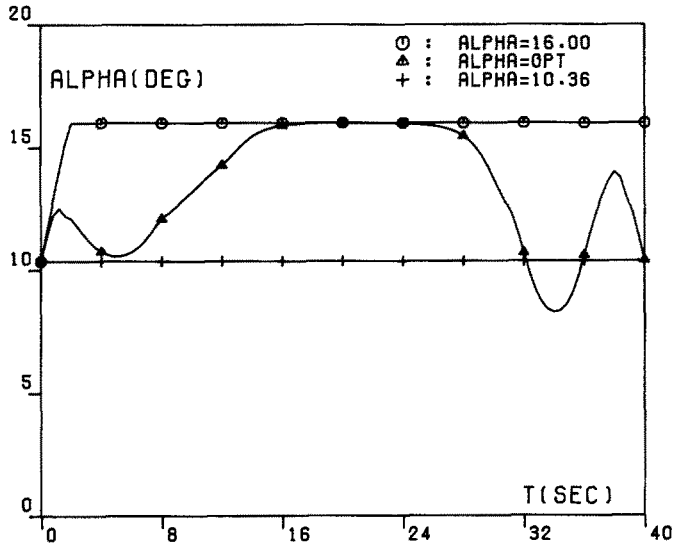

Fig. 7E. Relative angle of attack α versus time t (Case 3)

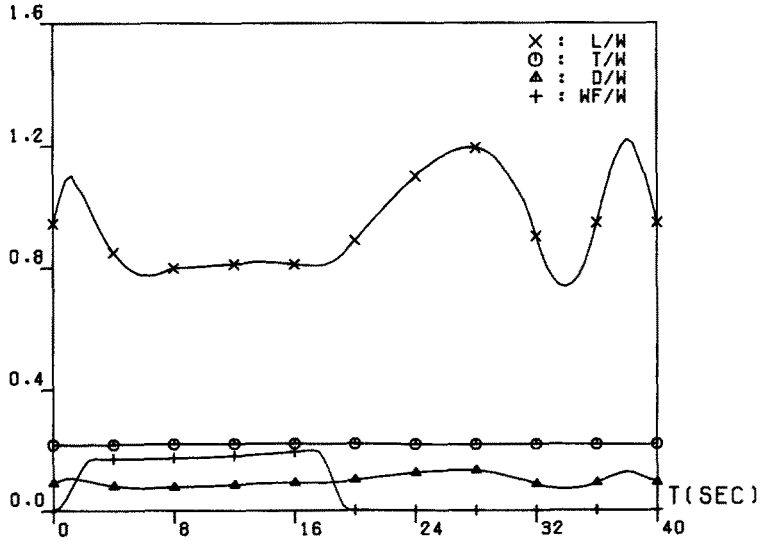

Fig. 7F. Lift-to-weight ratio L/W, thrust-to-weight ratio T/W, drag-to-weight ratio D/W, and windshear inertia force-to-weight ratio W_F/W versus time t (Case 3).

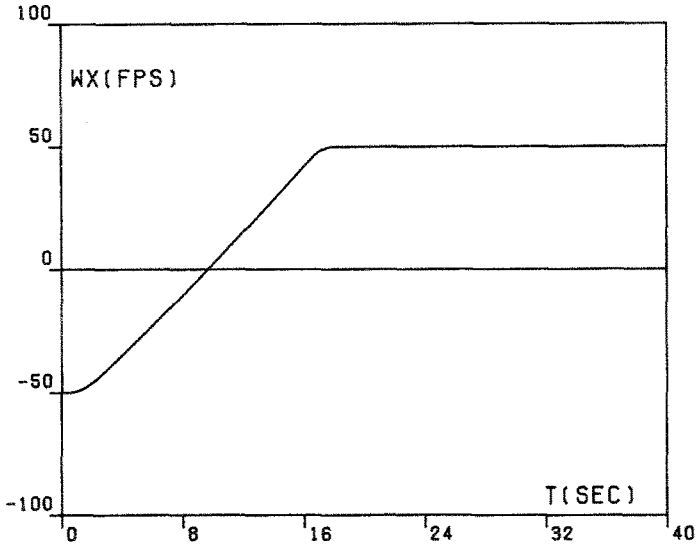

Fig. 8A. Horizontal component of the wind velocity W_x versus time t (Case 4).

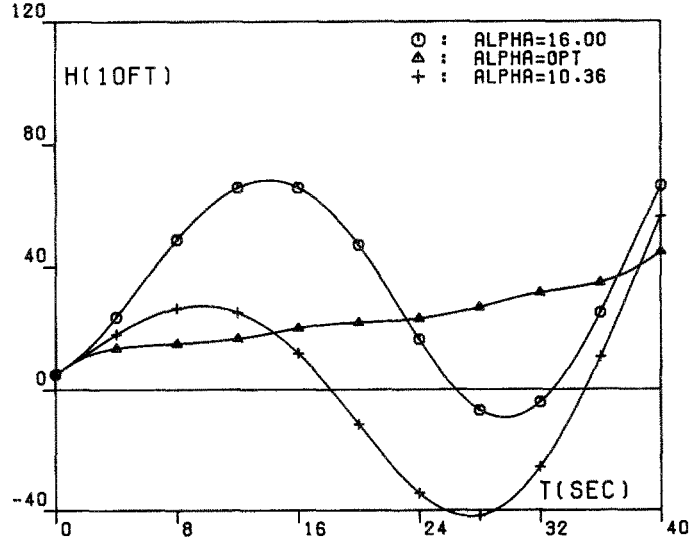

Fig. 8B. Altitude h versus time t (Case 4).

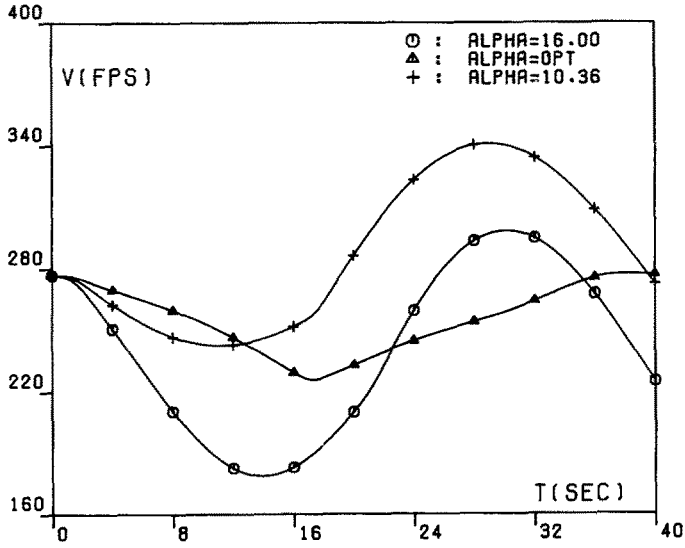

Fig. 8C. Relative velocity V versus time t (Case 4).

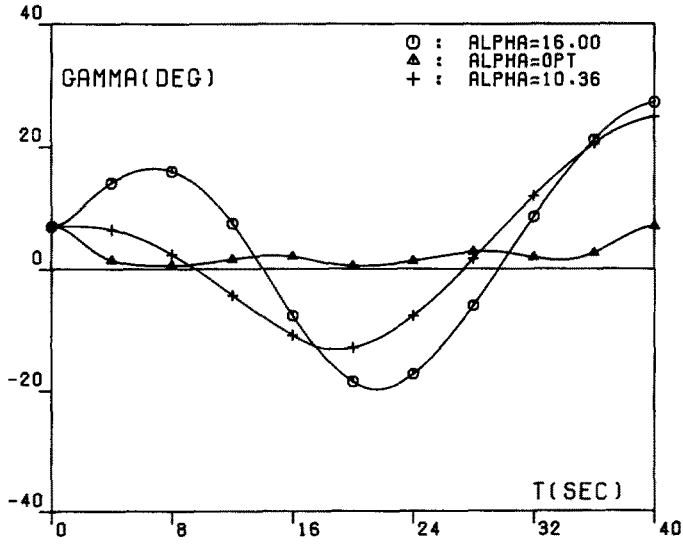

Fig. 8D. Relative path inclination γ versus time t (Case 4).

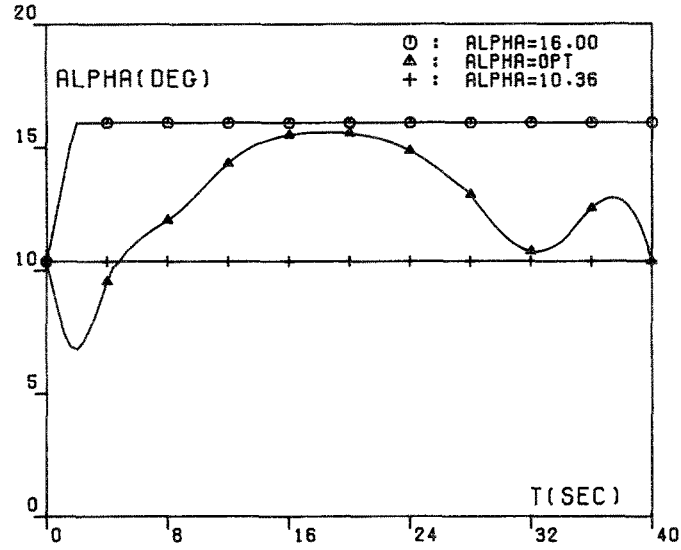

Fig. 8E. Relative angle of attack α versus time t (Case 4).

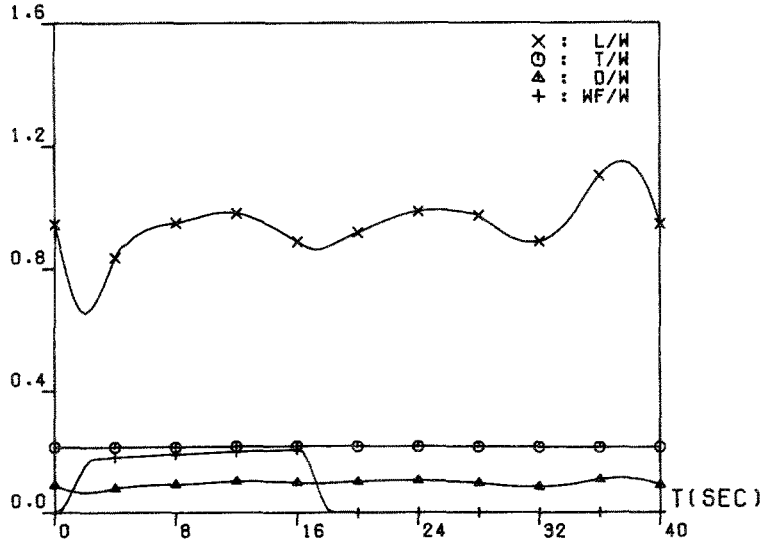

Fig. 8F. Lift-to-weight ratio L/W, thrust-to-weight ratio T/W, drag-to-weight ratio D/W, and windshear inertia force-to-weight ratio W_F/W versus time t (Case 4).

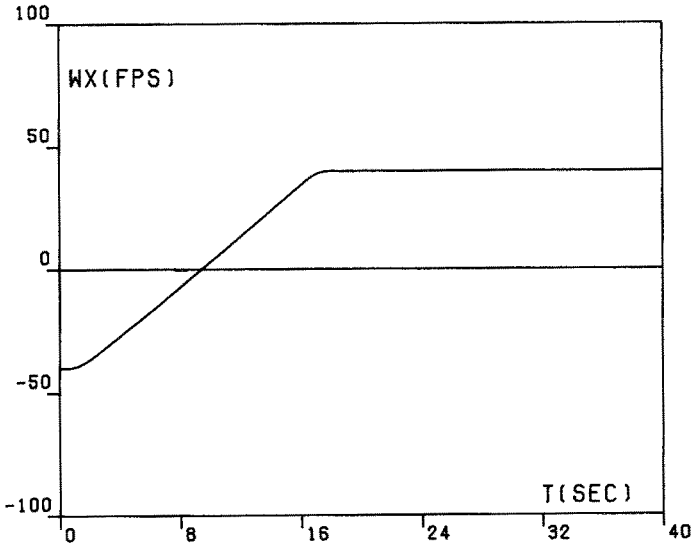

Fig. 9A. Horizontal component of the wind velocity W_x versus time t (Case 5).

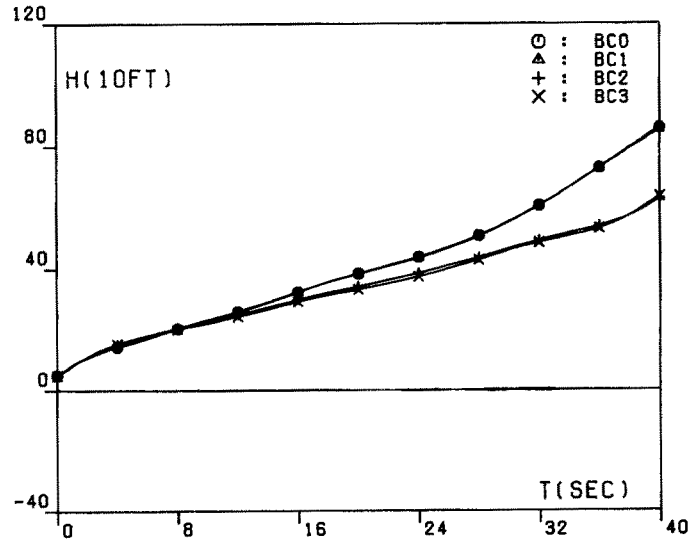

Fig. 9B. Altitude h versus time t (Case 5).

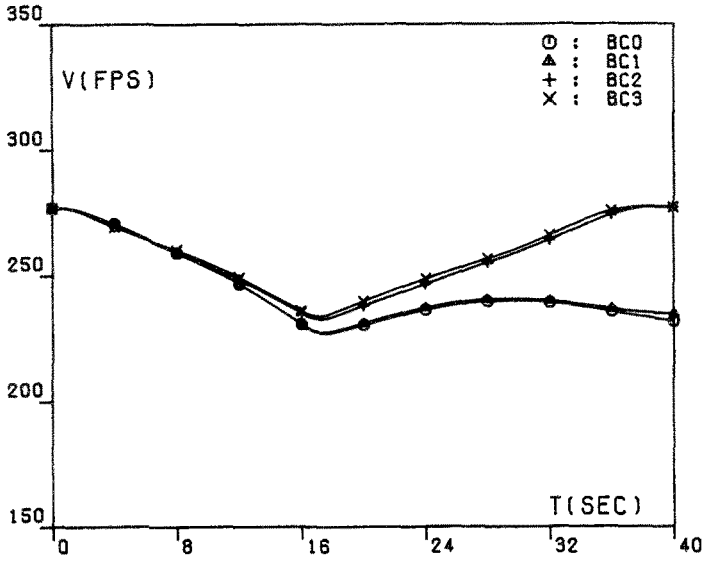

Fig. 9C. Relative velocity V versus time t (Case 5).

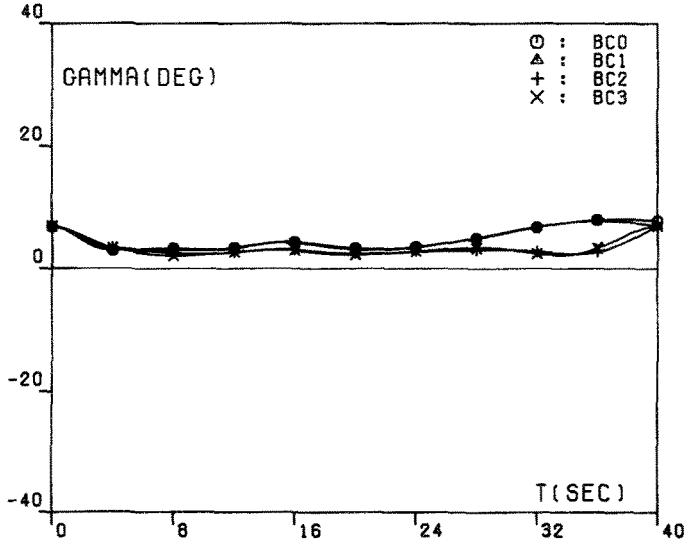

Fig. 9D. Relative path inclination γ versus time t (Case 5).

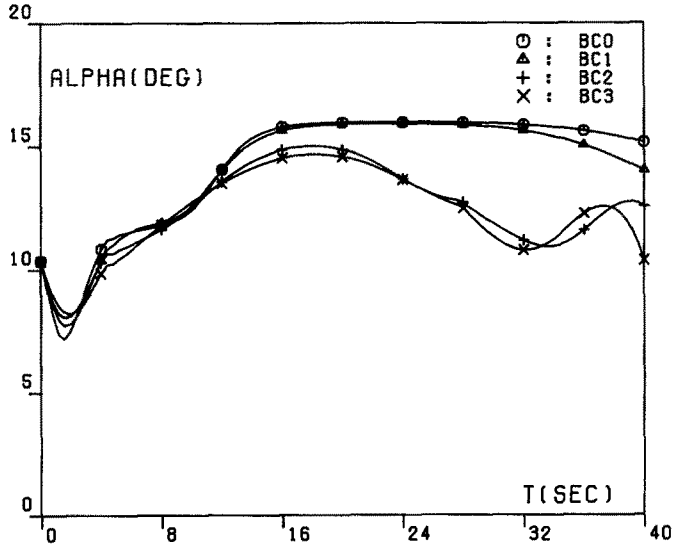

Fig. 9E. Relative angle of attack α versus time t (Case 5).

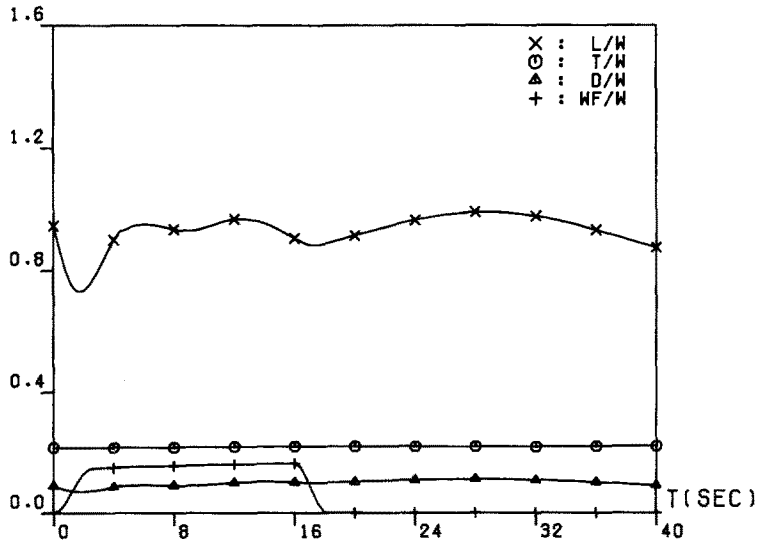

Fig.9F. Lift-to-weight ratio L/W, thrust-to-weight ratio T/W, drag-to-weight ratio D/W, and windshear inertia force-to-weight ratio W_F/W versus time t (Case 5, boundary condition model BC1).

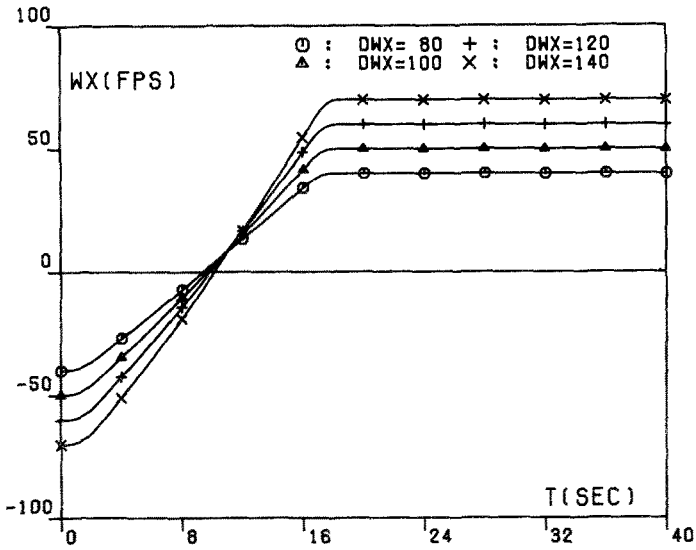

Fig. 10A. Horizontal component of the wind velocity W_x versus time t (Case 6).

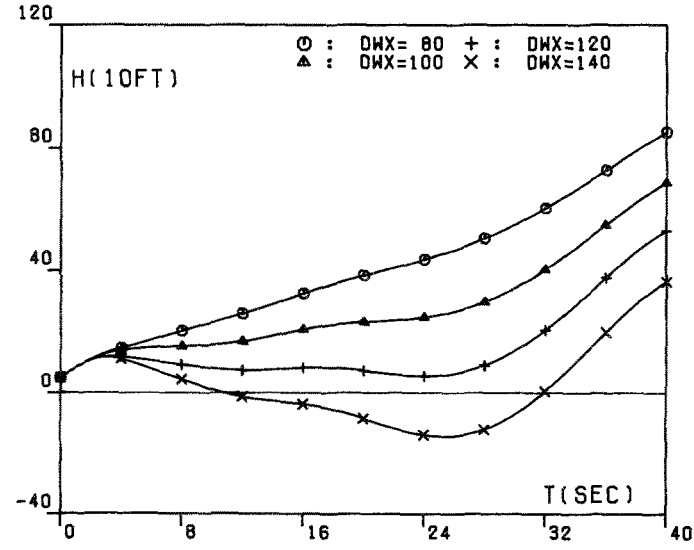

Fig. 10B. Altitude h versus time t (Case 6).

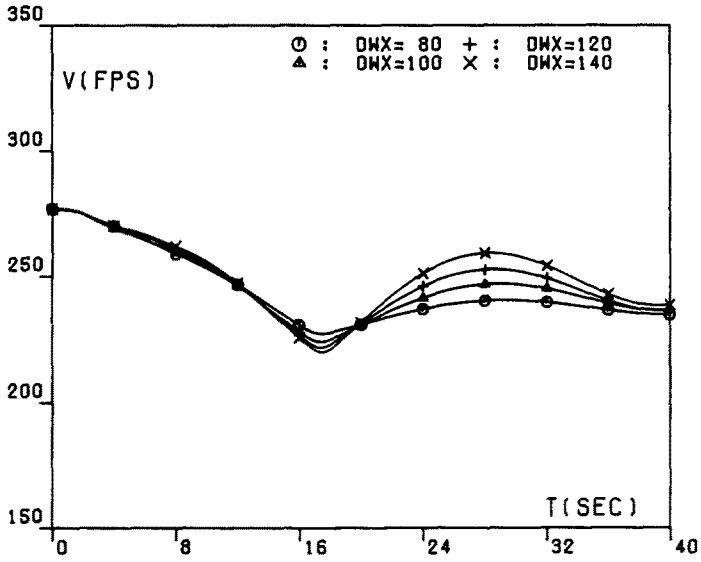

Fig. 10C. Relative velocity V versus time t (Case 6).

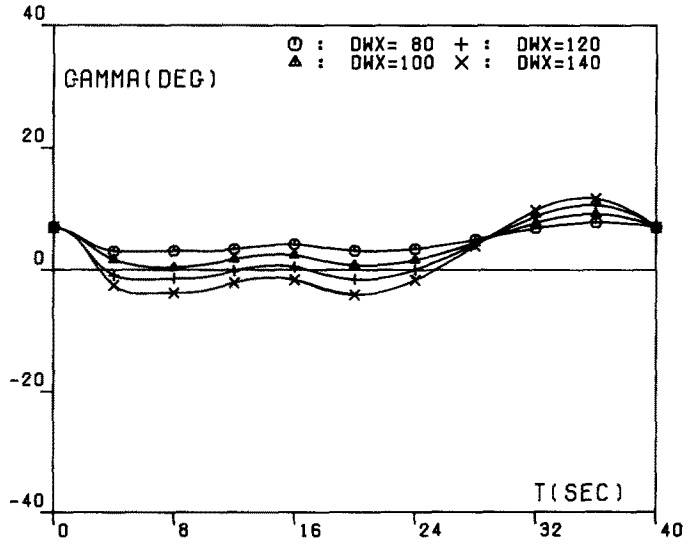

Fig. 10D. Relative path inclination γ versus time t (Case 6).

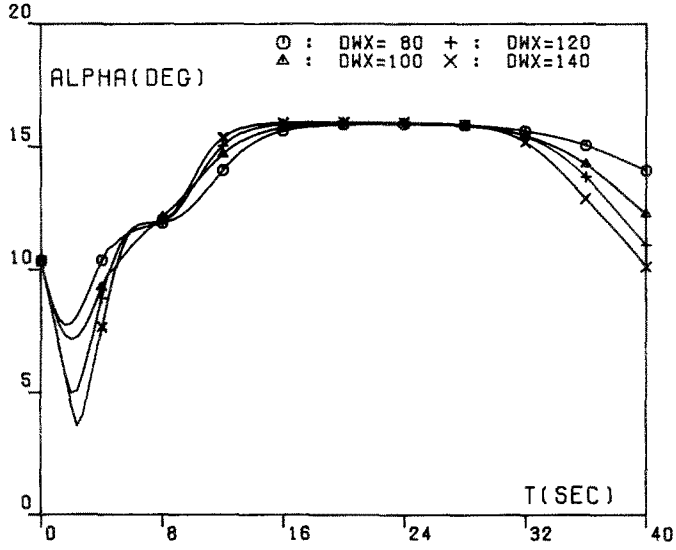

Fig. 10E. Relative angle of attack α versus time t (Case 6).

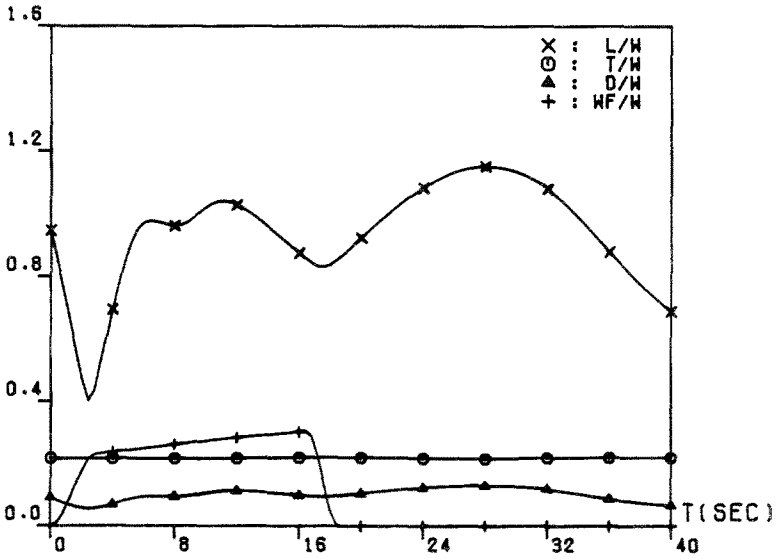

Fig. 10F. Lift-to-weight ratio L/W, thrust-to-weight ratio T/W, drag-to-weight ratio D/W, and windshear inertia force-to-weight ratio W_F/W versus time t (Case 6, wind velocity difference $\Delta W_x = 140$ ft sec^{-1}).